MENUS – Materials Engineering by Neutron Scattering

Ke An[1,a)], Alexandru D. Stoica[1], Thomas Huegle[2], Jiao Y.Y. Lin[1], Van Graves[3]

[1]*Neutron Scattering Division, Oak Ridge National Laboratory, Oak Ridge, TN 37831, USA*
[2]*Neutron Technology Division, Oak Ridge National Laboratory, Oak Ridge, TN 37831, USA*
[3]*Spallation Neutron Source Second Target Station Project, Oak Ridge National Laboratory, Oak Ridge, TN 37831, USA*

[a)]Author to whom correspondence should be addressed: kean@ornl.gov. Present address: Neutron Scattering Division Oak Ridge National Laboratory, 1 Bethel Valley Rd., Oak Ridge, TN 37831, USA. Telephone: +1-865-576-2185. Fax: +1-865-574-6080.

MENUS at STS will be a transformational high-flux, versatile, multiscale materials engineering diffraction beamline with unprecedented new capabilities for the study of complex materials and structures. It will support both fundamental and applied materials research in a broad range of fields. MENUS will combine unprecedented long-wavelength neutron flux and unique detector coverage to enable real-time studies of complex structural and functional materials under external stimuli. The incorporated small angle neutron scattering (SANS) and transmission/imaging capabilities will extend its sensitivity to larger length scales and higher spatial resolution. Multimodal MENUS will provide crystallographic and microstructure data to the materials science and engineering community to understand lattice strain/phase transition/microstructure/texture evolution in three orthogonal directions in complex material systems under combined extreme applied conditions. The capabilities of MENUS will open new scientific opportunities and meet the research needs for science challenges to enable studies of a range of phenomena and answer the key questions in material design/exploration, advanced material processing, transformative manufacturing, and material operations of national impacts in our daily life.

I. INTRODUCTION

Advanced structural and functional materials are widely used across many industries and applications, including nuclear energy, infrastructure, semiconductor, aerospace, transportation, and national security. The advantages of neutrons for studying engineering materials lie in their deep penetrating power, ability to monitor atomic-scale changes during actual operating and processing conditions, sensitivity to isotopic differences, and in many cases, high elemental contrast. The second target station (STS) at the Spallation Neutron Source, Oak Ridge National Laboratory provides unique opportunities for new instrumentation that is not currently available at the first target station (FTS). A multimodal materials engineering instrument concept as highlighted in the report "First Experiments: New Science Opportunities at the Spallation Neutron Source Second Target Station"[1] can be realized by the MENUS instrument discussed here.

MENUS, a next generation engineering materials diffractometer, takes the advantage of STS broad band cold neutron source to be a transformational high-flux, versatile, multiscale materials engineering beamline with unprecedented new capabilities for the study of low-symmetry, complex materials under in situ/operando conditions. It will support both fundamental and applied materials science and engineering research in a broad range of fields, including advanced alloy design[2, 3], energy storage and conversion[4, 5], nuclear energy[6], aerospace[7], transportation[8], and advanced manufacturing[9], etc. MENUS will combine unprecedented long-wavelength neutron flux and high detector coverage to enable real-time studies of complex structural and functional materials behavior under mechanical, thermal, electrical, and magnetic fields.

The instrument will incorporate small angle neutron scattering (SANS) and transmission/imaging capabilities to extend its sensitivity to larger length scales and higher spatial resolution. MENUS will allow simultaneous characterization of microstructures and phenomena across multiple length scales, including nucleation and growth of precipitates[10, 11], metastable and intermediate phases in complex alloys[10, 12, 13] and composite materials[14], long-range order[2] , and stress-induced charge-ordering[15] or defects[16] etc. With large out-of-plane detector coverage, high-spatial-resolution in situ stress/strain/chemistry/microstructure measurements can be performed rapidly at once; and in situ, full orientation distribution function (ODF)/stress-orientation distribution function (SODF)[17] can be recorded rapidly by rotating the sample around a single axis.

MENUS will complement the strengths of the current VULCAN engineering materials diffractometer at FTS [18, 19]. Specifically, in the Q-range matched to low-symmetry materials, MENUS will have a neutron flux up to 3 orders of magnitude higher than VULCAN can deliver because of the high cold neutron brightness available at STS. The capabilities on MENUS will open new scientific opportunities and meet the basic research needs for challenges (basic research needs for future nuclear energy and basic research needs for transformative manufacturing) [20, 21] to enable studies a wide range of phenomena and answer the

key questions [1, 21] in material design/exploration, advanced material processing, transformative manufacturing, and material operations of national impacts in our daily life [22].

II. CAPABILITY REQUIREMENTS AND TARGETED INSTRUMENT CHARACTERISTICS

A list of high-level capability requirements is presented below by including most expected and representative use of MENUS. The key instrument characteristics such as sampling size, beam divergence and wavelength range to support the capabilities are also envisioned as below.

A. High-level capability requirements

The design of the MENUS instrument is driven by the science cases, resulting in the following key requirements:

- Wide out-of-plane detector coverage to provide three-orthogonal-direction structural information simultaneously and large d-range coverage of diffraction lines under combined extreme fields.
- Open sample area and precision translation sample stage to accommodate various sample environments including loadframes with induction heating.
- Instrumental inventory must include special tools to achieve high sampling spatial resolution[23] and detectors for diffraction contrast[24] and transmission imaging[25].
- Instrument configuration must include a SANS setup to accommodate simultaneous multiscale dynamic studies[10, 11].
- Versatile exchangeable neutron optics required to switch between different experimental configurations for time-resolved or spatially resolved measurements.
- Sub-second data collection rate and live data streaming/analysis protocol as required for in situ or operando observations.

B. Types of experiments and instrumental configurations

MENUS will be designed for flexible instrument configurations including the following:

- Complete ODF, SODF, and microstructure characterization during in situ thermomechanical testing (high-intensity mode, 5 mm spatial sampling)
- Determination of full residual stress tensor in engineering components (high-intensity mode, 2 mm spatial sampling)
- In operando characterization of phase and microstructure evolution in functional devices under complex environmental conditions (high-intensity or high-resolution mode, 2 mm spatial sampling)

- Visualization of phase and elastic strain inhomogeneity by coded aperture pinhole neutron diffraction (high-intensity or high-resolution mode, 0.2 mm spatial sampling)
- Diffraction contrast tomography of single crystals and coarse-grained materials (high-resolution mode, <0.1 mm spatial sampling)
- Complementary transmission imaging/tomography of complex heterogeneous specimens (high-resolution, 0.1 mm spatial sampling)
- Simultaneous diffraction and SANS for kinetic studies (SANS–high-resolution mode)

C. Sampling size, beam divergence, and wavelength range

For neutron diffraction two instrument configurations are envisioned: high-intensity (HI) and high-resolution (HR) supporting the modes of operation described above. The high-intensity mode will permit fine tuning of neutron beam divergence and beam size at the sample position in the range of 0.3^o to 0.6^o and 1–25 mm^2 area, respectively. It will be dedicated to in situ studies of materials under external stimuli testing and residual stress mapping in complex engineering components. The high-resolution mode will provide a tight neutron beam angular divergence of 0.15^o and a larger beam area at the sample of about 4 cm^2. Moreover, this option will enable transmission and diffraction contrast neutron imaging. For simultaneous SANS and diffraction mode the dedicated optical arrangement will provide an angular divergence of 0.12^o within a beam cross section of 1 cm^2 at the sample position. A broad wavelength range of 1.5 Å to 12 Å is envisioned to support all possible experimental needs. Table 1 summarizes the key capabilities articulated.

Table 1 Key capability requirements for MENUS.

Parameter	Description
Beam size at sample	• 1×1 mm^2 to 5×5mm^2 (high-intensity mode) • ~4 cm^2 (high-resolution mode) • ~1 cm^2 (SANS-diffraction high-resolution mode)
Beam divergence	○ 0.3° to 0.6° (high-intensity mode) ○ ~0.15° (high-resolution mode) ○ ~0.12° (SANS-diffraction high-resolution mode)
Wavelength range	1.5 Å ≤ λ≤ 12 Å
Bandwidth (Δλ)	~3.5 Å (15 Hz), ~7.0 Å (7.5Hz)
d-spacing resolution	0.0008≤ Δd/d ≤ 0.0066 (depending on scattering angle and mode of operation)

In the following sections we focus on the physics design, engineering concept, and representative performance estimate to discuss the features of MENUS which meets the requirements above.

III. INSTRUMENT LAYOUT

The best choice for the MENUS beamline involves viewing the cylinder coupled para-hydrogen moderator of STS with a 3×3 cm^2 window. A sample-moderator distance of about 72 m is necessary to achieve the time of flight (TOF) wavelength resolution requirements. A single frame at 15 Hz will allow a bandwidth of ~3.5 Å, which is comparable to the effective bandwidth in use at VULCAN with 1/3 frame suppression (20 Hz). Due to the improved moderator brightness and the adequate repetition rate delivers a throughput gain of two orders of magnitude is expected in the d-spacing range greater than 2 Å. The maximum wavelength range expected to be used spans from 1 to 8 Å, at 7.5 Hz with ½ frame suppression, which corresponds to a d-spacing range of 0.5–7.9 Å (or 0.8–12.5 $Å^{-1}$ in Q-range) for the full diffraction detector coverage. Within the same wavelength band, the SANS detector will cover the small Q-range from $2x10^{-3}$ to 1.4 $Å^{-1}$.

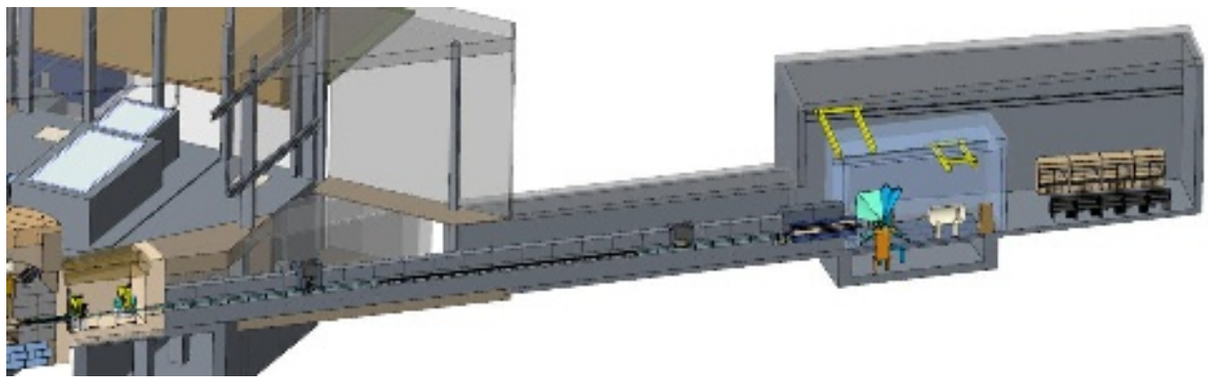

Figure 1. The overview of the MENUS beamline.

An overview of the engineering concept is presented in Fig. 1 and some end-station layout details are shown in Fig. 2. The beam delivery system will include two bandwidth definition choppers located inside STS bunker at 6.5 m and 10 m from the moderator. The guide system will efficiently deflect the cold neutron beam in order to completely prevent the direct view of the moderator from the instrument end-station. The first supermirror guide starts at about 7 m and ends at 54 m from the moderator. It delivers a deflected neutron beam at the secondary source location (63.75 m from the moderator), where a tunable aperture will allow to control the beam size. Three different secondary optics devices will be placed on an elevator system to be optionally used for different measurement configurations. A detailed description of

the secondary optics design is included in the next chapter. A tunable aperture will ensure the final beam conditioning just before the sample position and, by translating along the beam direction, will accommodate different sample environments. The 1 T capacity sample positioning stage located inside the end-station (Fig. 2(a)), with the center of rotation at 72 m from the moderator, will be surrounded by 5 detector banks with the working location at 3 m from the sample and a parking location for easy access to the sample environment. Convergent collimators will be placed in front of the detector banks to restrict the sampling area along the beam direction. The SANS detector in a vacuum tank will be located at 4.5 m downstream from the sample position.

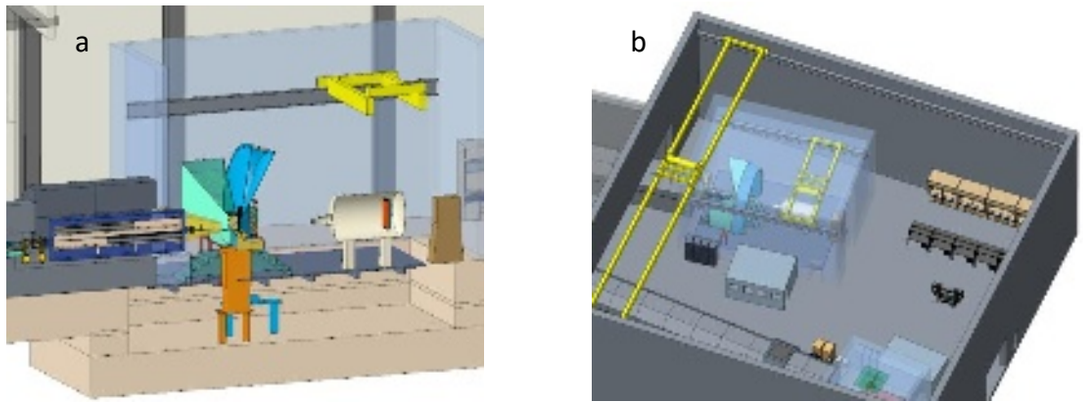

Figure 2. The conceptual design of multi-modal MENUS with its unique detector coverage (a) and the bay area for a materials science and engineering lab (b).

It is envisioned that the MENUS and EWALD[26] instruments will be included in a common building. MENUS will tackle problems beyond engineering materials; and it will serve the community as a materials characterization lab with multi-probe capabilities, including conventional probing techniques. As shown in the footprint of the instrument (Fig. 2(b)), space is reserved for ex situ tools with capabilities to investigate radiated samples, such as lapping machines, microscopes, furnaces, thermogravimetric analysis systems, dynamic mechanical analysis devices, resonant ultrasound spectrometers, and off-line mechanical load-frames.

IV. BEAM DELIVERY SYSTEM

A. Optics design

As the viewed moderator face is small, there is an opportunity to employ elliptic-shaped reflecting surfaces to deflect the neutron beam and create a rather concentrated secondary neutron source far from the moderator location. Moreover, as the beam divergence is expected to be the same in the horizontal and

vertical plane, the same deflection can be achieved in both directions by using the nested KB mirror concept[27], i.e. only two walls of the guide will be supermirror coated and the other two being neutron absorbent. To deliver the neutrons to the sample position, a second KB mirror will be positioned between the secondary source and the sample to deflect the neutron beam once more and reduce the background. Different types of mirrors, exchangeable via a translation stage, will be used to deliver high-intensity or high-resolution conditioned neutron beam. The schematic of the optical design is shown in Fig. 3.

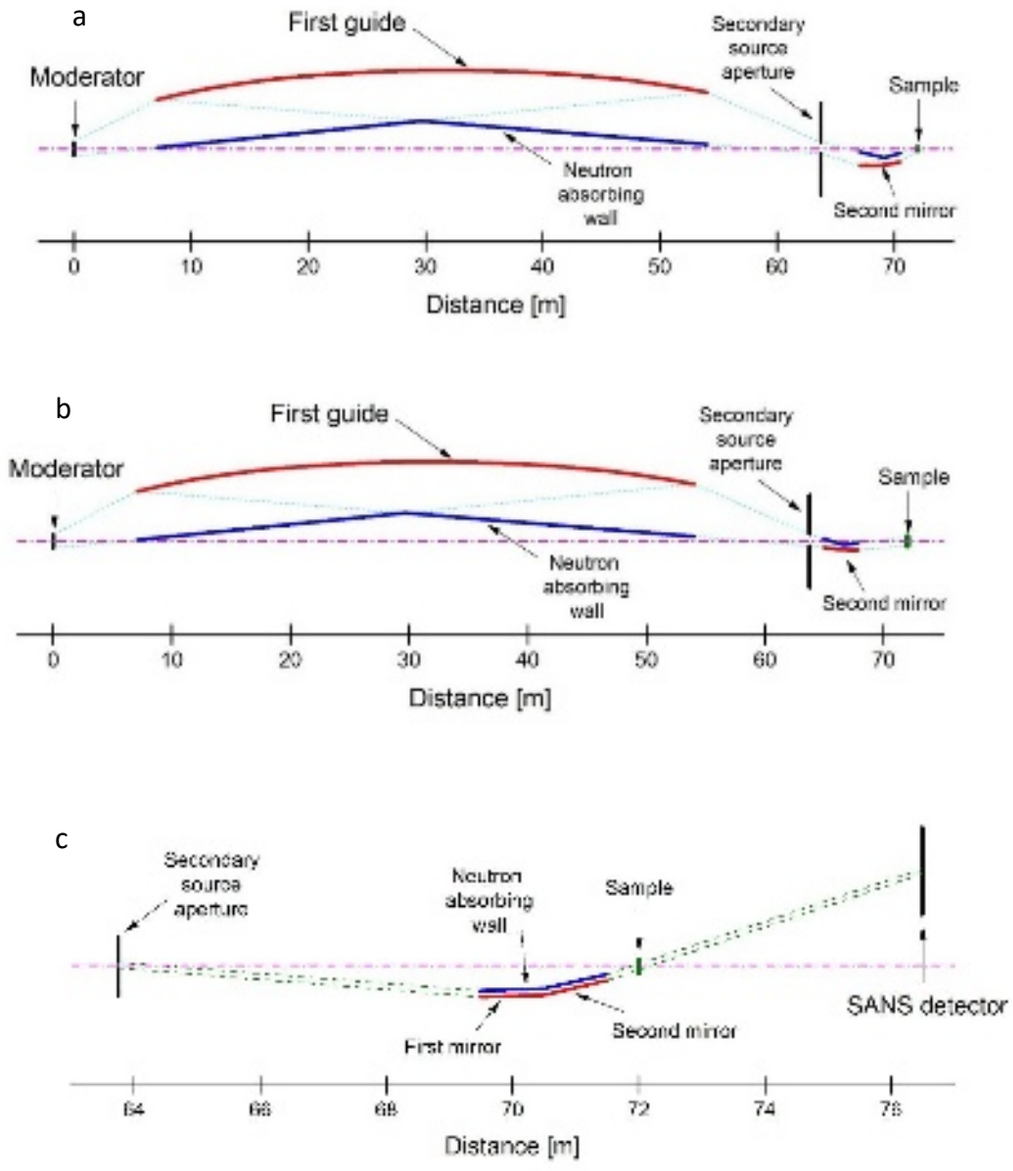

Figure 3. The neutron transport system of MENUS: (a) optics schematic for high-intensity option, (b) optics schematic for high-resolution option. (c) optics schematic for SANS option.

For the first two cases, in the section view along the beam, the horizontal and vertical shapes are identical, i.e. only one conceptual sketch is presented in Figure 3(a) and (b). The first elliptic mirror guide will start at 7.083 m from the moderator, and the displacement at the entrance will be 106.9 mm (left and up) from the nominal axis linking the center of the moderator with the center of the sample. The shape will be elliptic, with the ellipse foci located at the moderator center and at the secondary source, 63.75 m from the moderator. The exit will be at 54.025 m (46.9 m long) and 122.25 mm off axis. The supermirror will cover two sides of a neutron guide channel; on the sides opposite the mirror, the flat walls will not reflect neutrons; the channel width will decrease to about 100 mm at 29.65 m (all distances being from the face of the moderator). Thus, the nested KB mirror arrangement will act as a curved neutron guide; the only difference is that the number of reflections will be strictly reduced to two, one in the vertical and one in the horizontal plane. The phase space provided by the first neutron guide at the secondary source location (position versus divergence diagram) includes the acceptance phase space of all variants of the secondary optics, thus allowing for an efficient neutron transport to the sample position. A slit/monitor system located at the secondary source will allow the control of the beam size and the alignment of the secondary optics.

For high-intensity mode, a second KB mirror will start at 67.05 m and the displacement at the entrance will be 32.97 mm (Fig. 3(a)). The major axis of the second ellipse will be 6.75 m. The mirror will end at 70.5 m (1.5 m from sample position). At the exit, the displacement will be –25.54 mm. The smallest beam size inside the high-intensity guide will be 69.5 m (20.5 mm wide). This is the high-divergence configuration, which will provide a 5 by 5 mm^2 beam with a 0.6° divergence at the sample position. The divergence can be easily controlled by inserting two neutron absorber blades to reduce the beam cross section at the narrow guide location.

For the high-resolution option, the second KB mirror will start at 64.929 m and the displacement at the entrance will be –10.86 mm (Fig. 3(b)). The mirror will end at 67.875 m and the exit displacement will be –16.52 mm. The smallest beam size inside the high-resolution guide will be 66.575 m (9.8 mm width). This is the small divergence configuration, which will provide an 18 by 18 mm^2 beam with a 0.15° angular neutron beam divergence at the sample position.

For the SANS option, the optics must focus the beam at the detector position, which is facilitated by using a Wolter type mirror arrangement[28]. First an elliptic mirror will image the secondary source at a large distance and next a hyperbolic mirror will create a real image at the detector position (Fig. 3(c)). The sequence of two nested KB mirrors starts at 69.481 m and the displacement at the entrance will be –50.63 mm. The last mirror will end at 71.5 m and the exit displacement will be –22.88 mm. The smallest beam size inside the SANS guide will be at 70.5 m (11 mm wide). This configuration will provide an 8 by 8 mm^2

beam at the detector location with a 0.115° beam divergence. At the sample position the neutron beam footprint will reach 1 cm^2.

B. Neutron choppers and timing

The frame definition chopper functionality will be determined by the total neutron flight path, including moderator-sample (72 m) and sample-detector distance (3 m). The chopper timing graph is presented in Fig. 4. The first chopper (double disk) will be located at 6.5 m from the moderator and have a disk opening of about 34.7°. The double disk design will provide a reduced opening time and allow for changing the wavelength bandwidth, which is a feature required by some special applications. In addition to the working bandwidth, the first chopper will transmit slow neutrons (of about 40 Å); to absorb these unwanted neutrons, a second chopper with a disk opening of 52° will be placed 10 m from the moderator. A high-speed pulse-shaping chopper (not shown), with a duty cycle close to 50% (multiple openings), will be an optional way to achieve super-high resolution at the instrument. With the high-speed pulse shaping chopper located 6 m from the moderator and rotating at 300 Hz, the effective pulse width can be reduced to 25 μs, and the resolution in the backscattering detector bank is expected to be below 0.1%. In this mode of operation, the wavelength bandwidth will be reduced to 2.4 Å.

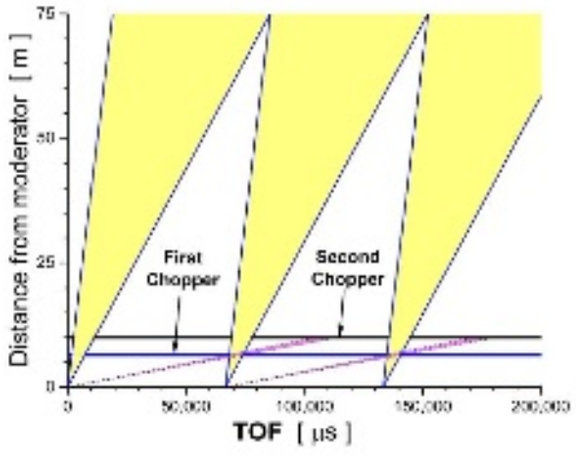

Figure 4. The MENUS chopper timing diagram.

C. Beam characteristics simulation by Monte Carlo model

The beam characteristics simulation for high-intensity, high-resolution and SANS options were performed by using a Monte Carlo model in the McStas code[29, 30]. They are shown in Fig. 5 and 6. The results for the high-intensity configuration are shown in Fig. 5. Fig. 5(a) shows the spatial distribution of

the neutron beam (with a wavelength larger than 1 Å). There is a quite homogeneous region of 5 by 5 mm^2, defined by an appropriate aperture located at 20 cm upstream from the sample position. Fig. 5(b) illustrates the corresponding divergence map for a 5 by 5 mm^2 beam extension. The beam extension and the angular distribution can be further controlled by the secondary source aperture and the narrowest cross section of the second KB guide, respectively.

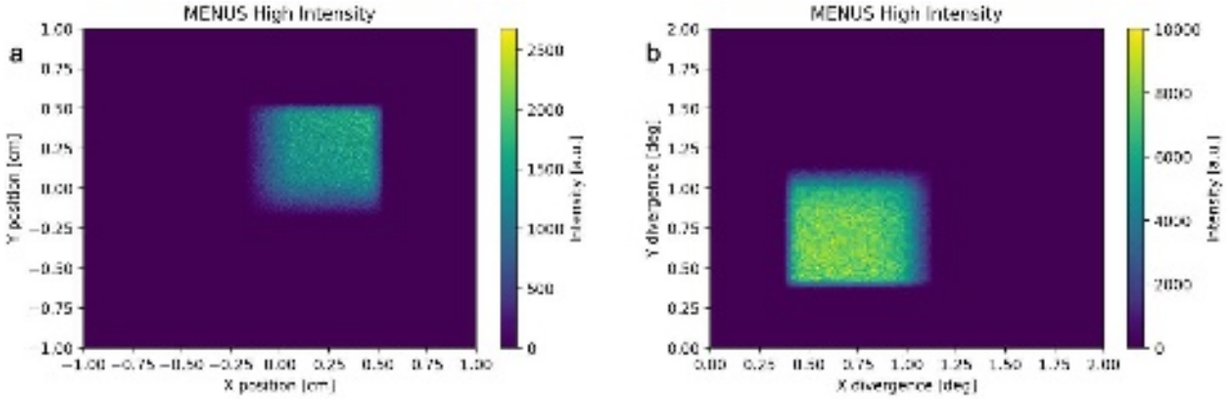

Figure 5. The results of McStas simulations of the high-intensity option for the MENUS neutron extraction system. a) features the total spatial distribution of neutrons at the sample position, and b) illustrates the resulting beam divergence map.

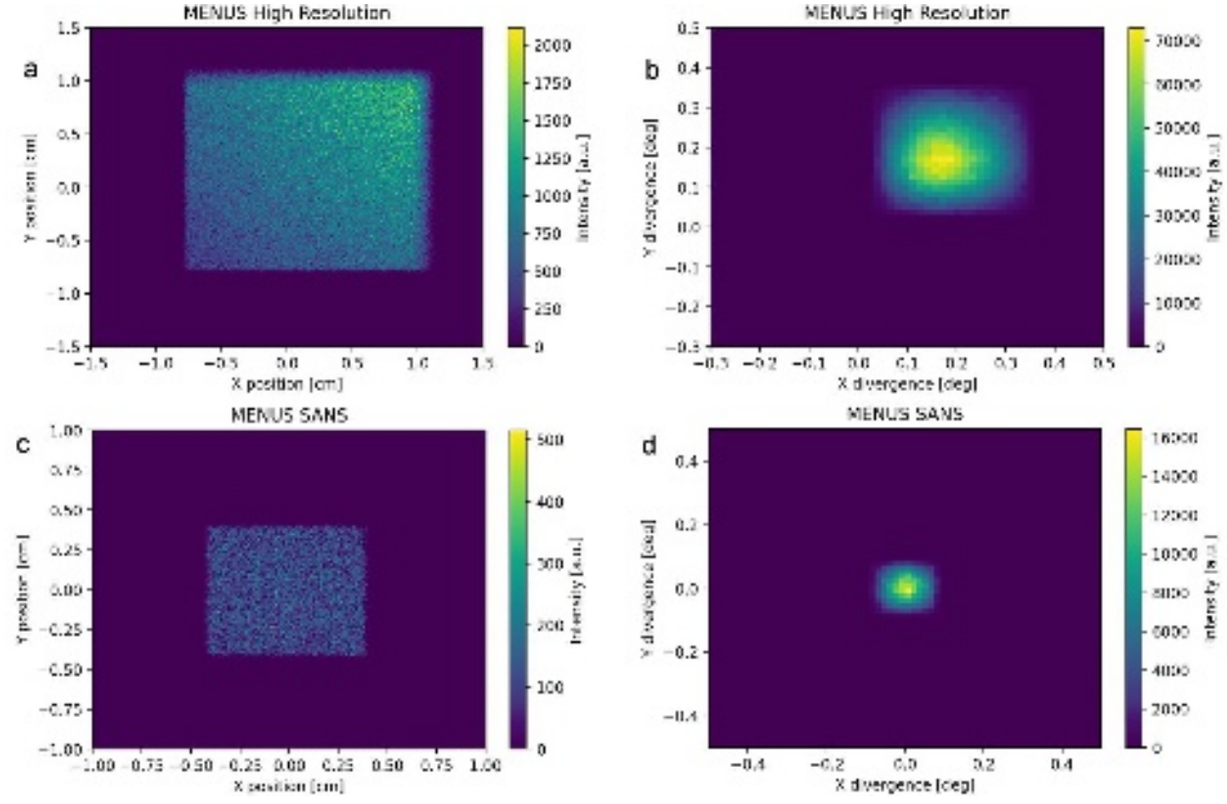

Figure 6. The results of McStas simulations of the two high-resolution options for the MENUS neutron extraction system. a) features the total spatial distribution of neutrons at the sample position for the high-resolution diffraction mode, and b) illustrates

the resulting beam divergence map. c) refers to the simultaneous SANS/diffraction option and d) features the beam spatial distribution and divergence at SANS detector location.

We summarize the results obtained for the high-resolution option in Fig. 6. In this case, an 18 by 18 mm^2 cross-section was obtained in Fig. 6(a). The beam divergence map, featured in Fig. 6(b), shows a distribution included in a 0.2^o square (0.15^o full width at half maximum), as opposed to about 0.6° for the high-intensity case in Fig. 5(b). The images in Fig. 6(c-d) summarize the simulation results for high-resolution SANS option. Fig. 6(c) refers to the neutron beam distribution at the SANS detector (4.5 m downstream from the sample position. It corresponds to a sharp 8 by 8 mm^2 cross section generated by the Wolter type sequence of mirrors, which allows for a clean imaging of a 9 by 9 mm^2 aperture located at the secondary source. The corresponding 0.115^o divergence (Fig. 6(d)) will allow for high quality SANS measurements simultaneously with collecting diffraction data.

The data presented in Fig. 5 and 6 refer to the neutron spectrum with wavelengths exceeding 1 Å. The divergence maps yield the expected performance of the beam. This neutron optics system will be very efficient at transporting the desired neutron phase space to the sample position, as shown in the brilliance ratio (defined as the ratio between the density in the phase space volume provided by the optical system at the sample position and the phase space density in the moderator) in Fig. 7. The results for neutron beam spectrum and resolution in diffraction are summarized in Section VI.

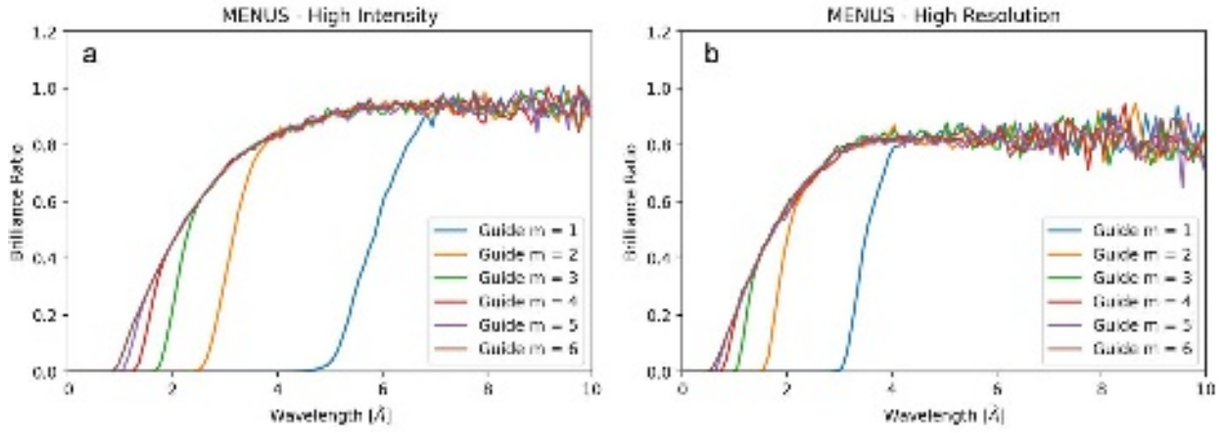

Figure 7. Brilliance ratio for two operating modes of MENUS, high-intensity (a) and high-resolution (b). beam conditions were as described in the text. Calculations were done for the indicated series of guide coatings. For simplicity, these coatings were used for the entire guide surface. Detailed optimization will use the highest index guide coatings only in the required locations.

V. DETECTORS LAYOUT

The conceptual sketch of the detectors layout is presented in Fig. 8(a) and (b). The circular detector bank (Fig. 8(a) in blue) contains a tilted array of 0.77 m long detector tubes positioned at a 70.5° scattering angle (from 61^o to 80°) and covering 250° of a conus centered on the nominal incident neutron beam direction and tangent to a 3 m radius sphere around the nominal sample location. Tight convergent collimators will limit the field of view along the beam direction to a 2 mm rage around the center of the sample positioning stage. The entire circular detector system can be displaced (retracted) along the beam to allow easy access to the sample stage.

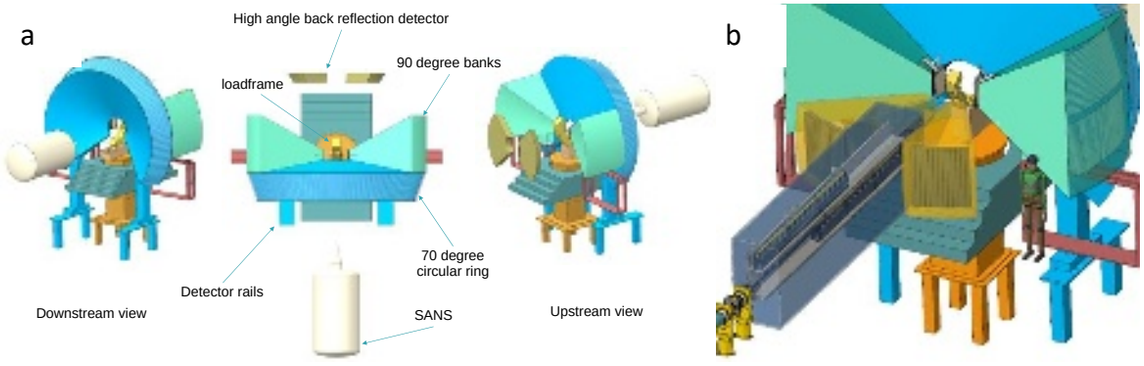

Figure 8. Three views of MENUS detectors layout (a) and the convergent collimators attached to them (b).

Two detector banks (Fig. 8(a) in green) will be positioned around ± 90^o scattering angles (from 80^o to 115°) and extend about 48° out of horizontal plane (from −15^o to 33°). Convergent collimators are also positioned in front of the detectors to restrict the field of view. Alternatively, for specific applications, the convergent collimator will be replaced by a coarse collimator with a coded aperture entrance. Each bank can be retracted away from the sample stage to allow easy access.

Additional detector banks (Fig. 8(a) in brown) will be deployed in backscattering from 150° to 170° and will be dedicated to high-resolution measurements required by special materials science problems when specific diffraction lines are too close to be separated in the usual configuration of the instrument. In combination with the pulse-shaping chopper, the backscattering detector will provide exquisite time-of-flight resolution (down to 0.08%) allowing to separate specific overlapping diffraction peaks, which may be essential to solve structural uncertainties. The back-reflection patterns will also offer excellent conditions for peak profile analyzes, which result in information about microstructural defects as dislocations, twins and grain boundaries. The convergent collimators associated to the backscattering banks are represented in Fig. 8(b). They also must be retractable together with their banks to allow accessing the secondary optics.

The coverage of the pole figure in the laboratory coordinates is presented in Fig. 9(a), as well as the pole figure coverage in specimen coordinates in Fig. 9(b), when the loading axis (LD) is tilted 54.74° from the vertical axis. The proposed detector configuration expedites diffraction analysis by measuring directly non-coplanar components of the strain, such as the three orthogonal strain components in LD, TD and ND directions as marked in red in Fig. 9, which are required for stress calculation; moreover, a complete determination of the ODF and SODF in polycrystalline samples can be performed by simply rotating the sample around a single (loading) axis by maximum 13 steps around the tilted loading direction specified in Fig. 9(b).

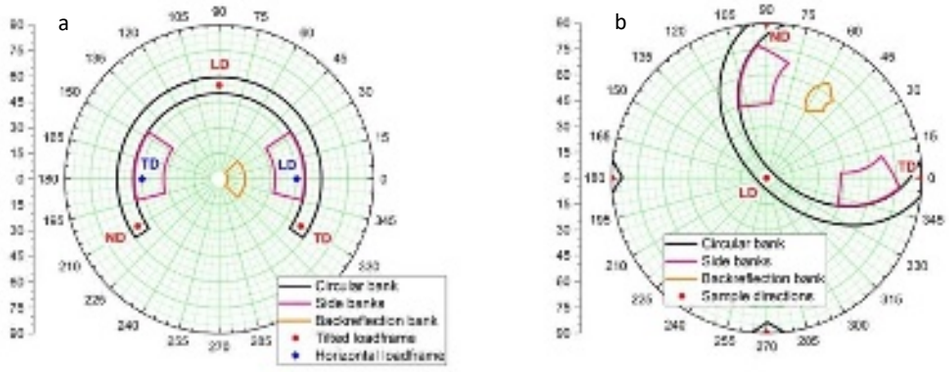

Figure 9. MENUS detector coverage. (a) detector coverage pole figure with beam at the center of the pole. (b) detector coverage in sample pole figure with the loading direction in the center of the pole.

The SANS detector (its vacuum tank featured in Fig. 8(a) in white), located at 4.5 m from the sample position, will allow simultaneous diffraction and SANS measurements for in situ kinetic phase transformation studies in functional materials and alloys[10]. The SANS pattern is especially useful in early stage of phase transformation when diffraction signal is too weak to allow quantitative determinations.

The high-resolution mode will support the use of small, high-spatial-resolution detectors (multi-channel plate (MCP) type with ~20 μm pixel size) to visualize the defect distribution within the specimen, as well as its grain morphology. In single crystals and coarse polycrystal specimens, the local lattice orientation can be determined and monitored in-situ by energy dispersive neutron transmission using MCP, simultaneously with the diffraction data acquisition. Alternatively, the MCP can be used in diffracted beam to determine the 3D grain structure of the specimen by diffraction contrast tomography[31]. MCP in transmission mode can be also used for fine grained specimens to visualize Bragg edges and monitor local texture changes[32, 33].

VI. PERFORMANCE ESTIMATE

The flux estimates from McStas[29] simulations are presented in Fig. 10. These estimates account for reflection losses from a supermirror m-factor of 6. Both flux values (per square centimeter) and total flux integrated over the useful beam areas are represented as functions of neutron wavelength. As a benefit of the coupled cold moderators of STS, MENUS has a significant gain at long wavelengths in flux, which peaks at 3.2×10^{8} n/cm^2·Å·s at ~λ=2.5 Å in high-intensity mode. This is compared with the neutron flux on the FTS VULCAN instrument as shown in Fig. 10, which peaks at ~λ=1 Å because the instrument views the decoupled, poisoned water (thermal) FTS moderator. VULCAN's neutron flux decreases quickly at long wavelengths, and the flux gain of MENUS at these long wavelengths can be several orders of magnitude (up to 3). The detailed comparison can be seen from Fig. 10. VULCAN has 7×10^{7} n cm^{-2} s^{-1} @ 30Hz 2MW HI Mode, while MENUS shows 6.4×10^{8} n cm^{-2} s^{-1} @ 15Hz 700kW HI Mode. VULCAN provides 0.6 Å to 5 Å useable wavelength, 1.44 Å bandwidth with 60 Hz; 2.88 Å bandwidth with 30Hz, and MENUS yields 1.5-12 Å useable wavelength, 3.5 Å bandwidth with 15Hz or 7Å bandwidth with 7.5Hz.

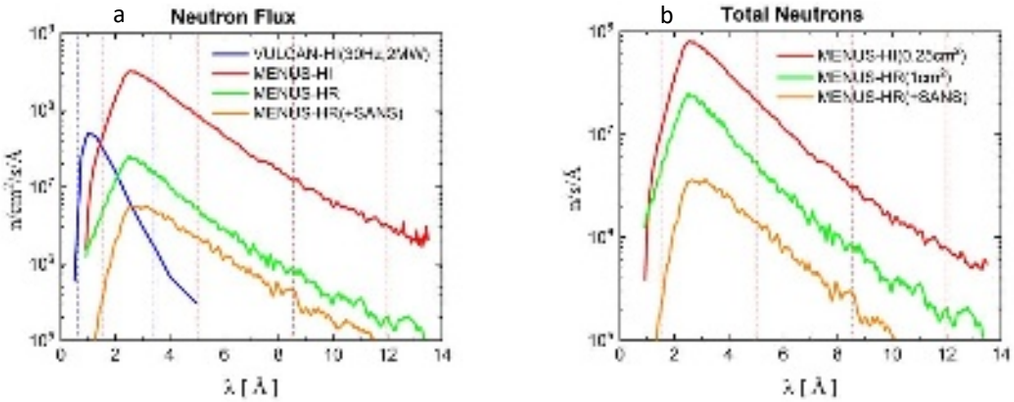

Figure 10. The neutron flux estimations derived from McStas simulations. a) Comparison of flux for VULCAN in high-intensity mode at 2 MW/30 Hz FTS future high-power stage and MENUS; the wavelength band boundaries for VULCAN are represented by blue dashed lines, whereas the possible wavelength bands for MENUS are delimited by red dashed lines; the total flux of VULCAN in its 2.88 Å band is 7.3x10^7 n/cm^2/s, as the estimated flux at MENUS in high-intensity mode for the 3 consecutive 3.5 Å band is: 6.4x10^8 n/cm^2/s (1.5-5 Å), 1.3x10^8 n/cm^2/s (5-8.5 Å), 2.3x10^7 n/cm^2/s (8.5-12Å). (b) Total neutrons on MENUS for specific options and their typical beam cross-sections; the integrated intensity over 3 consecutive bands are: HI - 1.6x108 n/cm^2/s (1.5-5 Å), 3.3x10^7 n/cm^2/s (5-8.5 Å), 5.6x10^6 n/cm^2/s (8.5-12Å) and HR – 4.6x10^7 n/cm^2/s (1.5-5 Å), 7.6x10^6 n/cm^2/s (5-8.5 Å), 1.7x10^6 n/cm^2/s (8.5-12Å); in the SANS option, the estimated values for two most likely to be used consecutive bands are: 8.3x10^6 n/cm^2/s (2-5.5 Å), 1.4x10^6 n/cm^2/s (5.5-9 Å).

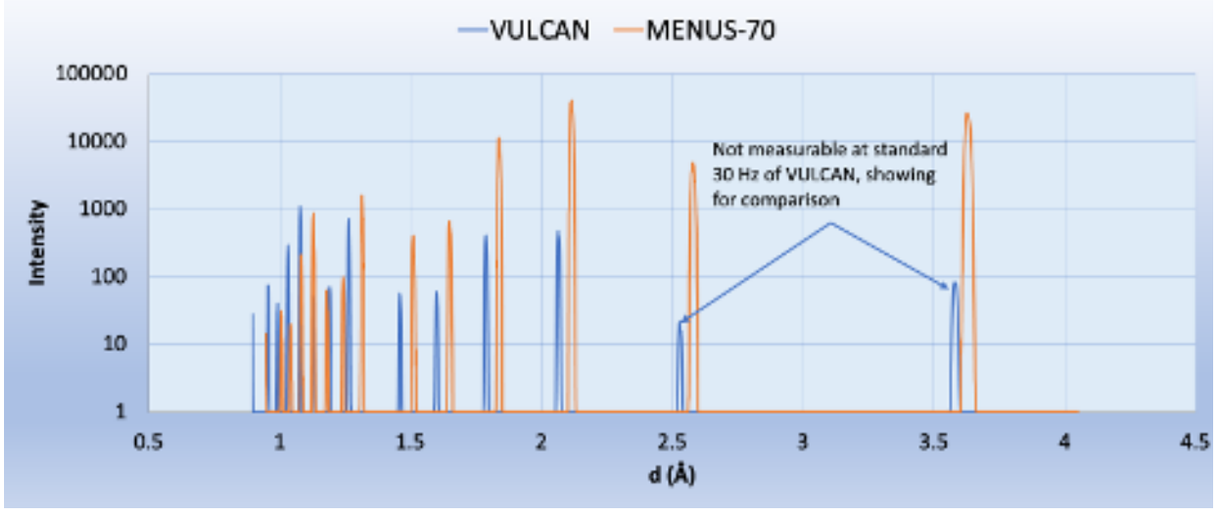

Figure 11. Comparison of diffraction intensity (log scale with base of 10) of VULCAN and MENUS 70° circular detector (data was shifted 0.05 Å to avoid peak overlaps). Note the change in vertical scale. (Both data sets are simulated with the same detector type and normalized to the same exposure time).

The performance of MENUS in measuring diffraction spectra was simulated using the McViNE code[34, 35] and is shown in Fig. 11 in comparison with that of VULCAN with 90° detector banks recording in a range of d spacings from 0.9 to 4 Å. The gain in instrument performance for measuring large d-spacing diffraction peaks is phenomenal. MENUS will excel at measuring large lattice or superlattice peaks rapidly, as shown clearly by the gain in the first two (large d-spacing) peaks (100, 110) of the simulated Ni_3Al ($L1_2$ super structure) diffraction patterns in Fig. 11.

*Table 2. List of instrument resolution configuration (*Δd/d *in %).*

Modes	**Circular bank** (61-80º)	**Side banks** (80-115º)	**Back banks** (150-170º)	**Back banks with pulse shaping**
HI (0.6º)	0.46-0.66	0.27-0.46	0.14-0.17	0.09-0.16
HI (0.45º)	0.37-0.52	0.23-0.37	0.14-0.16	0.08-0.13
HR	0.24-0.34	0.17-0.24	0.14	0.08-0.09
HR+SANS	0.22-0.31	0.16-0.22	0.14	0.08

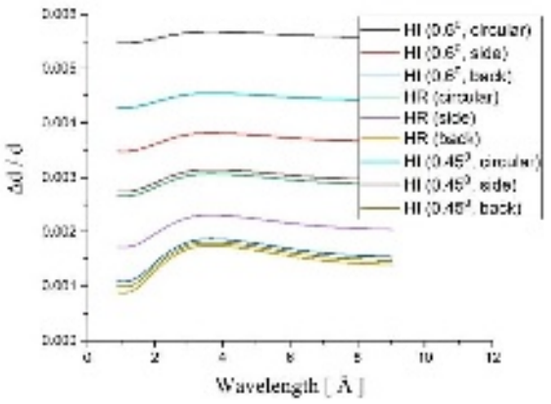

Figure 12. Versatile instrument resolution configurations in diffraction on MENUS, the resolution wavelength dependence with different divergences (0.6-HI, 0.45-HI, 0.15-HR) and detector angles (160-back, 90-side, 70-circular).

The Δd/d resolution of MENUS, estimated under a Gaussian approximation, has a broad range from 0.08% in super-high-resolution mode using the optional pulse-shaping chopper to average 0.56% for circular bank in high-intensity mode as demonstrated in Fig. 12. The wavelength dependence proved to be rather week and the range of average values are presented in Table 2. This capability will provide insight into challenging materials engineering problems to resolve closed and complex systems, and it provides much needed sensitivity for defect analysis such as dislocation density dynamic evolution during thermo-mechanical deformation, processing, and advanced manufacturing, etc.

The performance of the SANS option of MENUS was simulated by using the SANS_SPHERES component in McStas[29, 30]. The 1mm thick model sample has a neutron transmission of 95% and consists of 500 Å radius spheres with a volume fraction of 10% and excess scattering length density 0.6 fm/ Å^3. The first wavelength band (2-5.5 Å) was used in simulations, which imposed a lower cutoff in the SANS spectrum at 5x10^{-3} Å^{-1} due to the extension of the incident beam at the detector position. The SANS spectrum is presented in Fig. 13(a); the total number of neutrons scattered in the 6x10^{-3} Å^{-1} to 10^{-1} Å^{-1} interval amounts to 25000 n/s, which potentially allows for recording a SANS spectrum in a few minutes.

To test the spatial resolution capabilities of the quasi-parallel neutron beam in neutron imaging, the SANS option was considered. To this purpose, a 50-arms neutron absorbent rosette was placed at the sample position and a finely pixelated detector (20 μm) was placed at 20 mm after the sample. The image resulting from simulations is shown in Fig. 13 (b). As the rosette's arms can be distinguished up to 1 mm radius, it can be concluded that the spatial resolution is better than 60 μm, which matches the expected spatial

resolution of MCP detectors. Thus, the MCP detectors can be successfully used to visualize 100 μm details in both transmitted and scattered beam, provided that they can be positioned close enough to the sample.

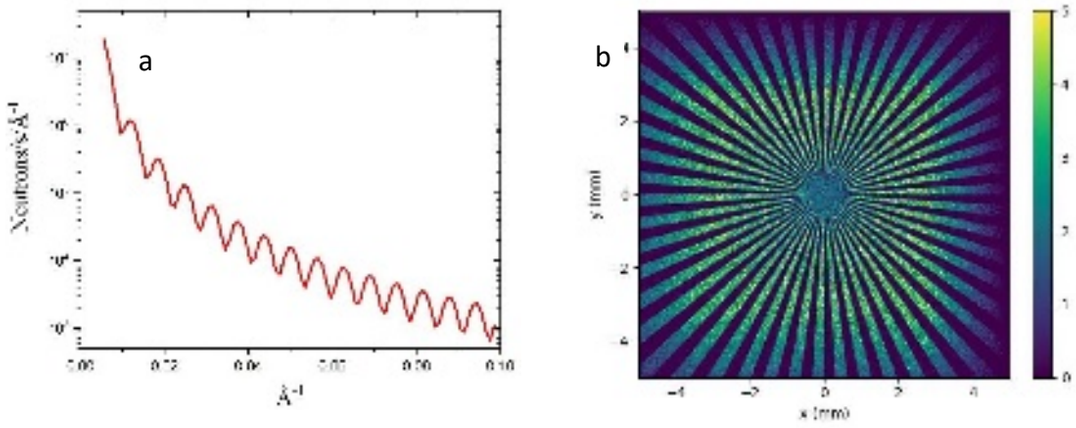

Figure 13. SANS and neutron imaging simulation results illustrating the complementary capabilities of MENUS to be used in experiments simultaneously with diffraction. a) simulated SANS pattern from a standard sample; b): the simulated neutron image in transmission of standard specimen used for resolution calibration.

We highlight the main differences of MENUS and VULCAN in the Table 3. Because the VULCAN moderator is optimized for thermal neutrons, the instrument has very limited long-wavelength neutrons, which challenge its ability to measure at large d-spacings. MENUS provides extended capabilities by the benefit of the unique characteristics of the STS and its novel detector layouts, while VULCAN is still a state-of-the-art engineering diffractometer for the study of high-symmetry materials with the requirement of high intensity at a shorter d-spacing. Once MENUS is built, the two instruments will provide complementary capabilities to the materials and engineering community.

Table 3. A comparison of main aspects of MENUS and VULCAN

ASPECTS	**VULCAN**	**MENUS**
Moderator	30x30 cm^2 high-resolution water moderator @FTS	3×3 cm^2 para-hydrogen moderator @STS
Source frequency	60 Hz	15 Hz
Avg. Flux (n cm^{-2} s^{-1})	7.3×10^7 @ 30Hz 2MW HI Mode	6.4×10^8 @ 700kW HI Mode
Incident energy	0.6 – 5 Å, 1.44 Å bandwidth @ 60 Hz; 2.88 Å bandwidth @ 30 Hz	1.5-12 Å, 3.5 Å bandwidth @ 15 Hz or 7Å bandwidth @ 7.5 Hz
Flight Path	43.75m	72m
Typical beam size	V: 1 – 12 mm H: 1 – 12 mm	V: 1 – 5 mm H: 1 – 5 mm
Detector type	Wavelength-shifting-fiber scintillation detectors 700x400 mm^2 (152x7pixels)	770 mm or 1000 mm long ^{3}He detector (6Hx5V mm^2)

Detector banks	±90° banks	±90° banks, ±150° high angle banks 70^{o} circular detector with 240^{o} degree coverage, SANS 1x1m^2 detector at 4.5m, 25x25 mm^2 MCP with 20 μm pixel size.
Collimation	2 or 5 mm	2 or 5 mm, 0.25 mm for PIND
Instrument resolution (broadening)	~0.25% @HR, ~0.5% @HI	Wide range of selection in resolution (0.08~0.66%) with pulse shaping chopper, and selectable beam divergence.
Multimodality	Simultaneous measurement in Q1, Q2, orthogonal; limited and slow Bragg transmission measurement	Simultaneous measurement in Q1, Q2 and Q3 orthogonal; rapid simultaneous SANS and quick Bragg transmission measurement to enable simultaneous crystallographic and microstructure investigations.
Main application examples	Residual stress, texture, phase and lattice strains in simple symmetry lattice (e.g. FCC/BCC). In-situ thermomechanical deformation, processing, synthesis, etc.	In-situ texture, strain ODF, nucleation, phase transformation, and anisotropic/ complex stress in low symmetry lattice (e.g. HCP/ orthorhombic), superlattice structure, magnetic ordering, battery, and multiscale probing in complex operando/processing systems, such as operando phase formation/transformations and stress development during additive manufacturing.

VII. SUMMARY

We have presented here a next generation powerful materials and engineering instrument. MENUS instrument is equipped with multimodalities of diffraction, SANS and imaging by using novel neutron optics and unique detector layout and offers versatile operation modes for different scientific and engineering areas. The performance estimate included here is to manifest some of the enabled representative features of the instrument at STS in terms of fluxes at different guide modes, representative diffraction, SANS in desired Q range, and imaging spatial resolution by using a standard rosette imaging gauge. However, this is not a complete list of what MENUS can do. Additional features, such as high spatial resolution pin hole diffraction imaging or Bragg edge/dip time-of flight neutron transmission, also take advantage of the unique characteristics of STS to complement the imperative research needs of user communities. MENUS will complement the strengths of the current VULCAN engineering materials diffractometer that uses the high wavelength resolution of thermal neutrons available at the FTS to study high-symmetry crystal structures in engineering materials and components. Specifically, in the Q-range matched to low-symmetry materials, MENUS will have a neutron flux up to 3 orders of magnitude higher than VULCAN can deliver because of the high cold neutron brightness available at STS. Multimodal MENUS will provide neutron scattering data with high temporal and spatial resolution to the materials science and engineering community to understand lattice strain/phase transition/microstructure/ texture evolution in three orthogonal directions in

complex material systems under combined extreme applied conditions including stress, temperature, and electric and/or magnetic fields. It will open new scientific opportunities for material exploration, material processing, and material operations. MENUS is expected to be one of the most impactful neutron instruments at ORNL to solve fundamental and applied problems by broad user communities.

ACKNOWLEDGMENTS

This research used resources of the Spallation Neutron Source Second Target Station Project and Spallation Neutron Source at Oak Ridge National Laboratory (ORNL), a DOE Office of Science User Facility operated by the Oak Ridge National Laboratory.

This manuscript has been authored by UT-Battelle, LLC under Contract No. DE-AC05-00OR22725 with the U.S. Department of Energy. The United States Government retains and the publisher, by accepting the article for publication, acknowledges that the United States Government retains a non-exclusive, paid-up, irrevocable, worldwide license to publish or reproduce the published form of this manuscript, or allow others to do so, for United States Government purposes. The Department of Energy will provide public access to these results of federally sponsored research in accordance with the DOE Public Access Plan (http://energy.gov/downloads/doe- public-access-plan)

[1]*First Experiments: New Science Opportunities at the Spallation Neutron Source Second Target Station*, (ORNL, 2019).
[2]T. Yang, Y. L. Zhao, Y. Tong, Z. B. Jiao, J. Wei, J. X. Cai, X. D. Han, D. Chen, A. Hu, J. J. Kai, K. Lu, Y. Liu and C. T. Liu Science **362,** (2018).
[3]H. Yang, D. Yu, Y. Chen, J. Mu, Y. D. Wang and K. An Mat Sci Eng a-Struct **680,** (2017).
[4]H. D. Liu, Y. Chen, S. Hy, K. An, S. Venkatachalam, D. N. Qian, M. H. Zhang and Y. S. Meng Adv Energy Mater **6,** (2016).
[5]L. Cai, K. An, Z. L. Feng, C. D. Liang and S. J. Harris J Power Sources **236,** (2013).
[6]C. A. Calhoun, E. Garlea, R. P. Mulay, T. A. Sisneros and S. R. Agnew Acta Mater **85,** (2015).
[7]S. Y. Huang, K. An, Y. Gao and A. Suzuki Metall Mater Trans A **49a,** (2018).
[8]Z. C. Sims, O. R. Rios, D. Weiss, P. E. A. Turchi, A. Perron, J. R. I. Lee, T. T. Li, J. A. Hammons, M. Bagge-Hansen, T. M. Willey, K. An, Y. Chen, A. H. King and S. K. McCall Mater Horiz **4,** (2017).
[9]B. Dutta, S. S. Babu and B. Jared, *Technology and Applications of Metals in Additive Manufacturing* (Elsevier, 2019).
[10]Y. Yang, T. Y. Chen, L. Z. Tan, J. D. Poplawsky, K. An, Y. L. Wang, G. D. Samolyuk, K. Littrell, A. R. Lupini, A. Borisevich and E. P. George Nature **595,** (2021).
[11]F. Ren, R. Schmidt, J. K. Keum, B. S. Qian, E. D. Case, K. C. Littrell and K. An Appl Phys Lett **109,** (2016).
[12]O. Benafan, R. D. Noebe, S. A. Padula, II, D. J. Gaydosh, B. A. Lerch, A. Garg, G. S. Bigelow, K. An and R. Vaidyanathan Scripta Materialia **68,** (2013).
[13]J. L. Lin, K. An, A. D. Stoica and B. J. Heuser J Nucl Mater **487,** (2017).
[14]K. Lin, W. J. Li, C. Y. Yu, S. H. Jiang, Y. L. Cao, Q. Li, J. Chen, M. H. Zhang, M. Xia, Y. Chen, K. An, X. B. Li, Q. H. Zhang, L. Gu and X. R. Xing Acta Mater **198,** (2020).
[15]Y. Chen, D. J. Yu and K. An Materials Research Letters **5,** (2017).
[16]Q. Xie, Z. Yan, D. Yu, K. An, X. Yan, S. Yin, B. Gillham, X. Wu, P. Yang, Z. Zhao and Y. Wang Acta Mater **226,** (2022).
[17]Y. D. Wang, X. L. Wang, A. D. Stoica, J. W. Richardson and R. L. Peng J Appl Crystallogr **36,** (2003).
[18]K. An, Y. Chen and A. D. Stoica Mrs Bull **44,** (2019).
[19]K. An, H. D. Skorpenske, A. D. Stoica, D. Ma, X. L. Wang and E. Cakmak Metall Mater Trans A **42a,** (2011).
[20]*Basic Reserach Needs workshop for Future Nuclear Energy*, (DOE BES, 2017).
[21]*Basic Research Needs for Transformative Manufacturing-Fundamental science to revolutionize manufacturing*, (DOE BES, 2020).
[22]*A remoarkable Return on investment in Fundamental Research-40 Years of Basic Energy Sciences at the Department of Energy*, (DOE BES, 2018).

[23]W. Wu, A. D. Stoica, K. D. Berry, M. J. Frost, H. D. Skorpenske and K. An Appl Phys Lett **112,** (2018).
[24]A. King, P. Reischig, J. Adrien, S. Peetermans and W. Ludwig Mater Charact **97,** (2014).
[25]N. Kardjilov, A. Hilger, I. Manke, M. Strobl, M. Dawson and J. Banhart Nucl Instrum Meth A **605,** (2009).
[26]L. Coates and L. Robertson J Appl Crystallogr **50,** (2017).
[27]G. E. Ice, R. I. Barabash and A. Khounsary Proc Spie **7448,** (2009).
[28]B. Khaykovich, M. V. Gubarev, Y. Bagdasarova, B. D. Ramsey and D. E. Moncton Nucl Instrum Meth A **631,** (2011).
[29]P. K. Willendrup, L. Udby, E. Knudsen, E. Farhi and K. Lefmann Nucl Instrum Meth A **634,** (2011).
[30]P. K. Willendrup, E. Farhi, E. Knudsen, U. Filges and K. Lefmann Journal of Neutron Research **17,** (2014).
[31]S. Samothrakitis, M. Raventos, J. Capek, C. B. Larsen, C. Grunzweig, M. Tovar, M. Garcia-Gonzalez, J. Kopecek, S. Schmidt and M. Strobl Scientific Reports **10,** (2020).
[32]L. L. Dessieux, A. D. Stoica, P. R. Bingham, K. An, M. J. Frost and H. Z. Bilheux Nucl Instrum Meth B **459,** (2019).
[33]L. L. Dessieux, A. D. Stoica and P. R. Bingham Rev Sci Instrum **89,** (2018).
[34]J. Y. Y. Lin, H. L. Smith, G. E. Granroth, D. L. Abernathy, M. D. Lumsden, B. Winn, A. A. Aczel, M. Aivazis and B. Fultz Nucl Instrum Meth A **810,** (2016).
[35]J. Y. Y. Lin, F. Islam, G. Sala, I. Lumsded, H. Smith, M. Doucet, M. B. Stone, D. L. Abernathy, G. Ehlers, J. F. Ankner and G. E. Granroth J Phys Commun **3,** (2019).

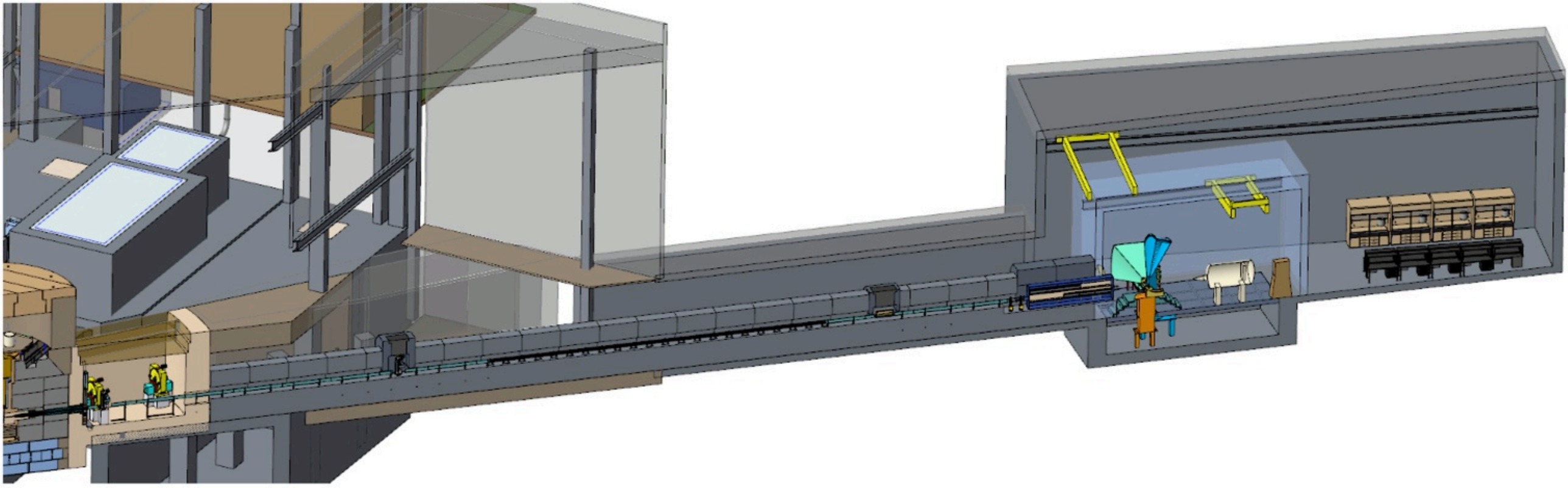

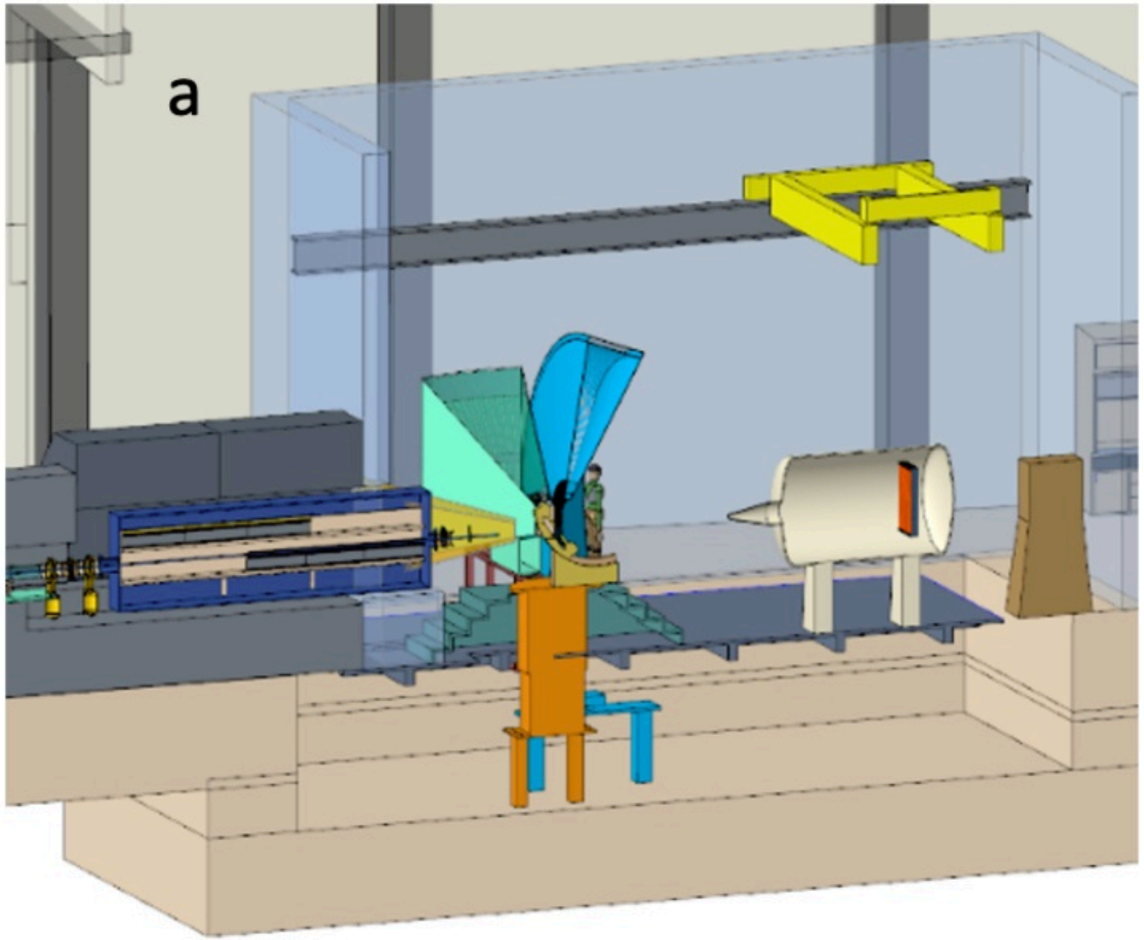
a

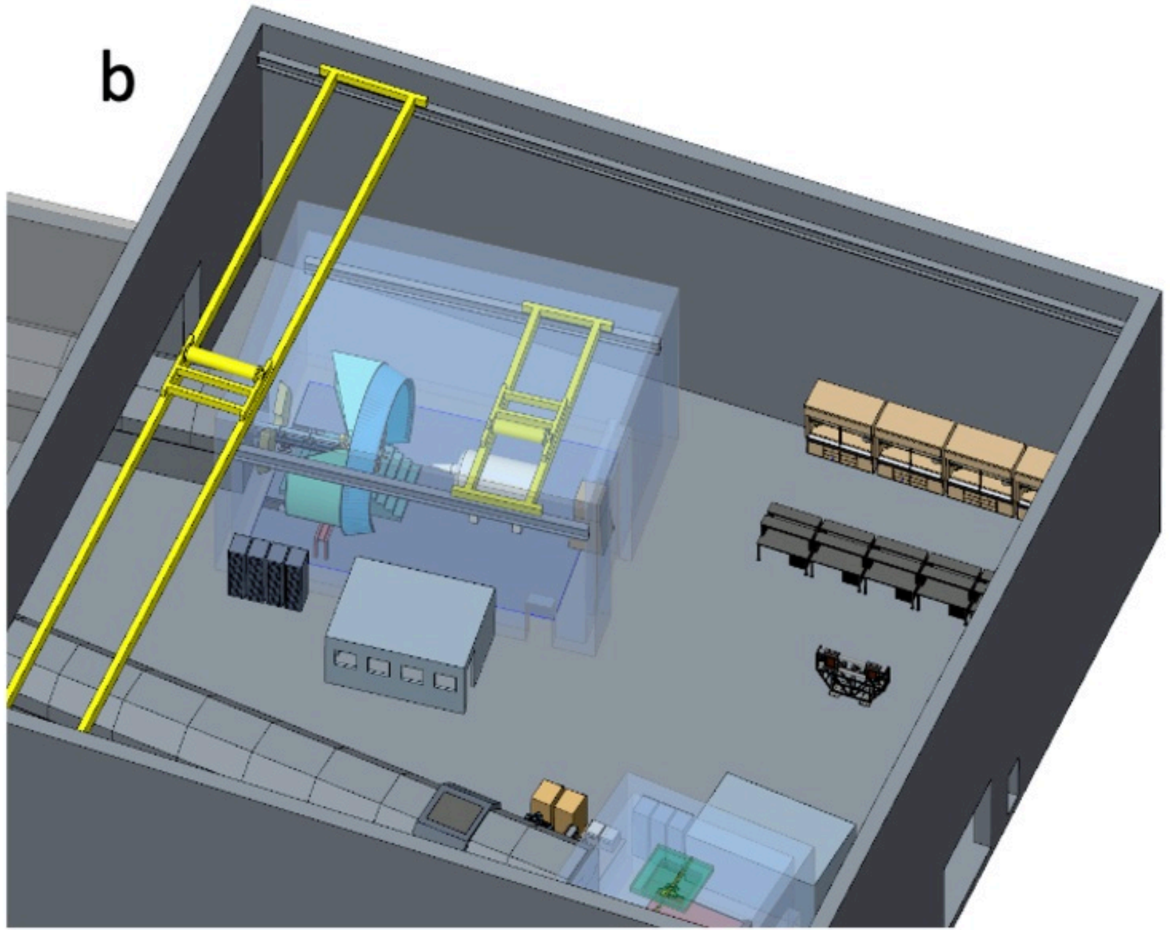
b

a

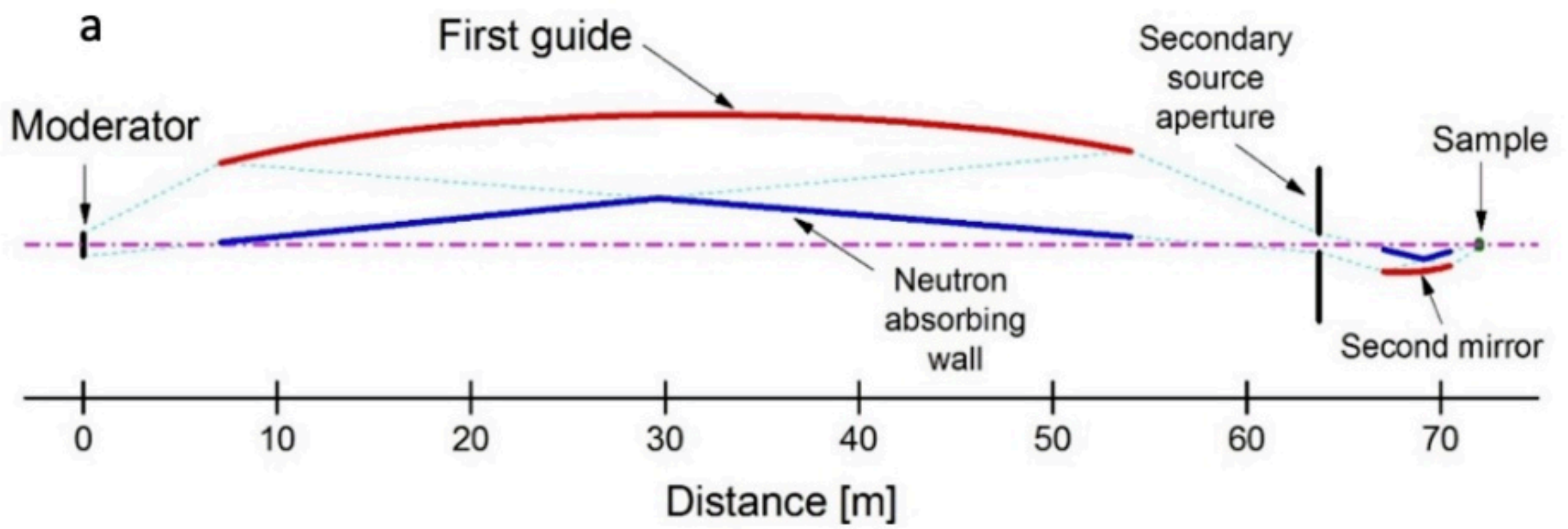
First guide
Secondary source aperture
Moderator
Sample
Neutron absorbing wall
Second mirror
0
10
20
30
40
50
60
70
Distance [m]

b

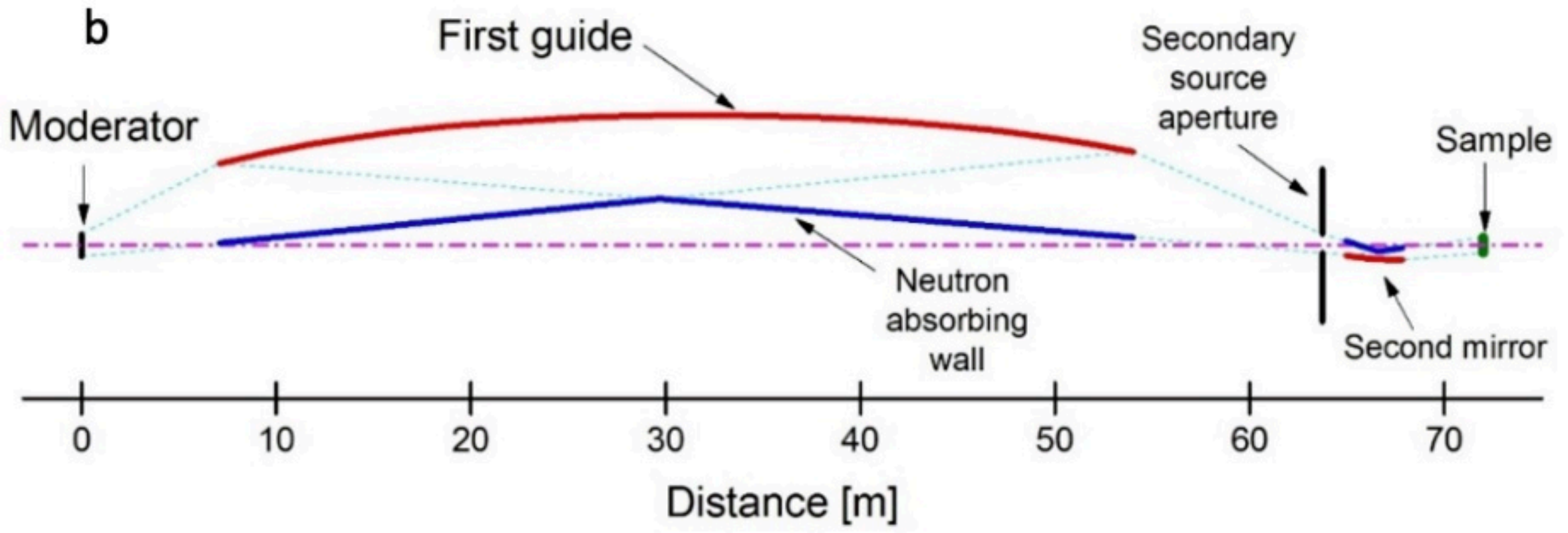
First guide
Secondary source aperture
Moderator
Sample
Neutron absorbing wall
Second mirror
0
10
20
30
40
50
60
70
Distance [m]

c

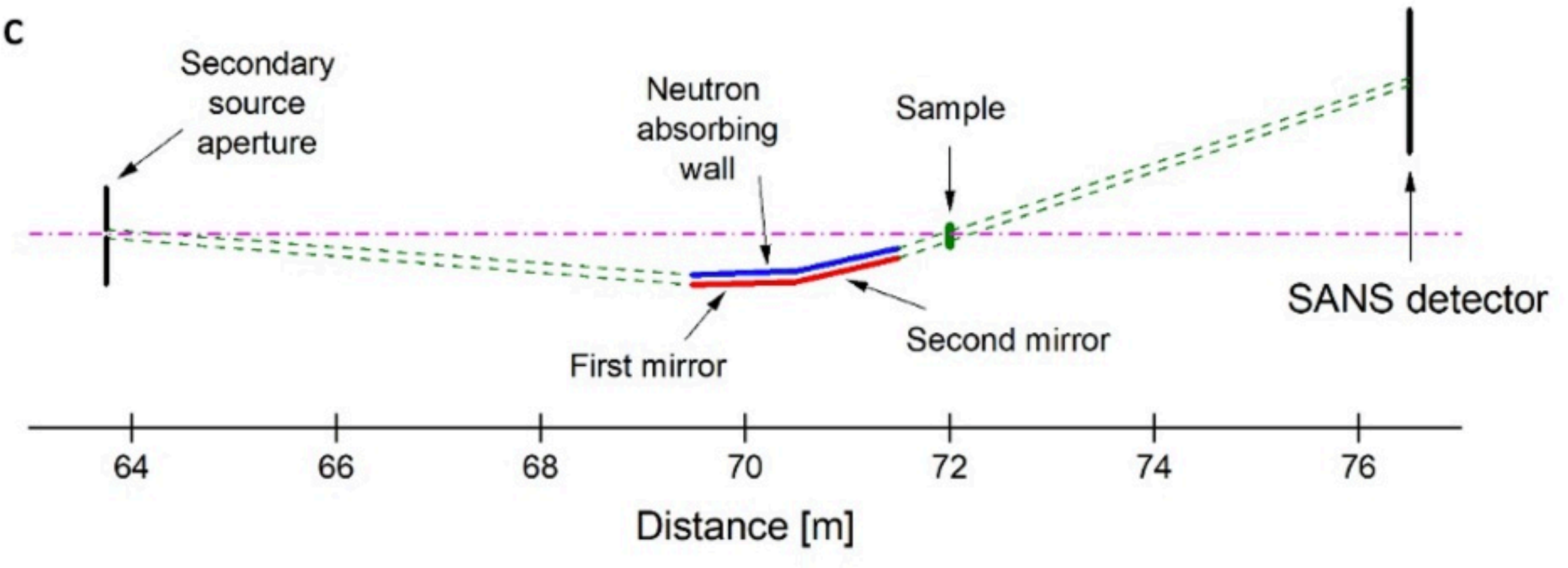
Secondary source aperture
Neutron absorbing wall
Sample
SANS detector
First mirror
Second mirror
64
66
68
70
72
74
76
Distance [m]

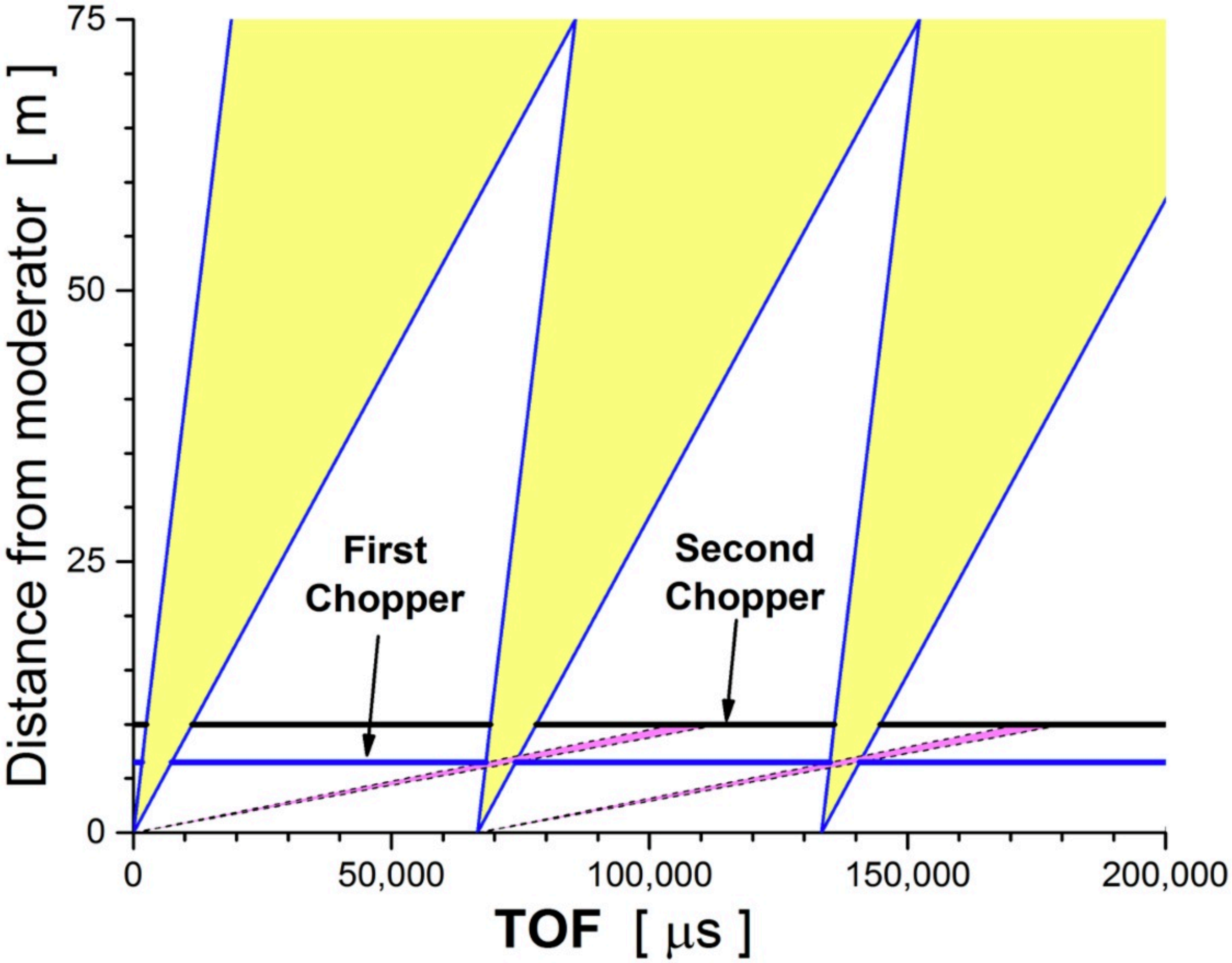
Distance from moderator [m]
75
50
25
0
First
Chopper
Second
Chopper
0
50,000
100,000
150,000
200,000
TOF [μs]

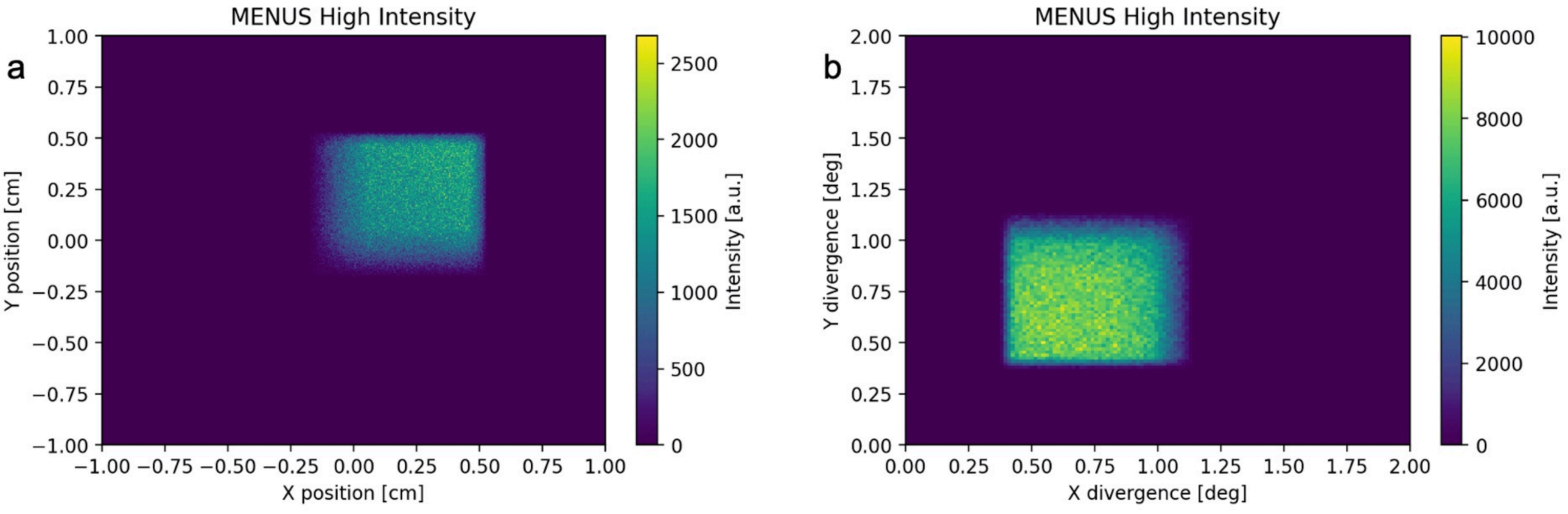
a
MENUS High Intensity
Y position [cm]
X position [cm]
Intensity [a.u.]
1.00
0.75
0.50
0.25
0.00
−0.25
−0.50
−0.75
−1.00
2500
2000
1500
1000
500
0
b
MENUS High Intensity
Y divergence [deg]
X divergence [deg]
Intensity [a.u.]
2.00
1.75
1.50
1.25
1.00
0.75
0.50
0.25
0.00
10000
8000
6000
4000
2000
0

a

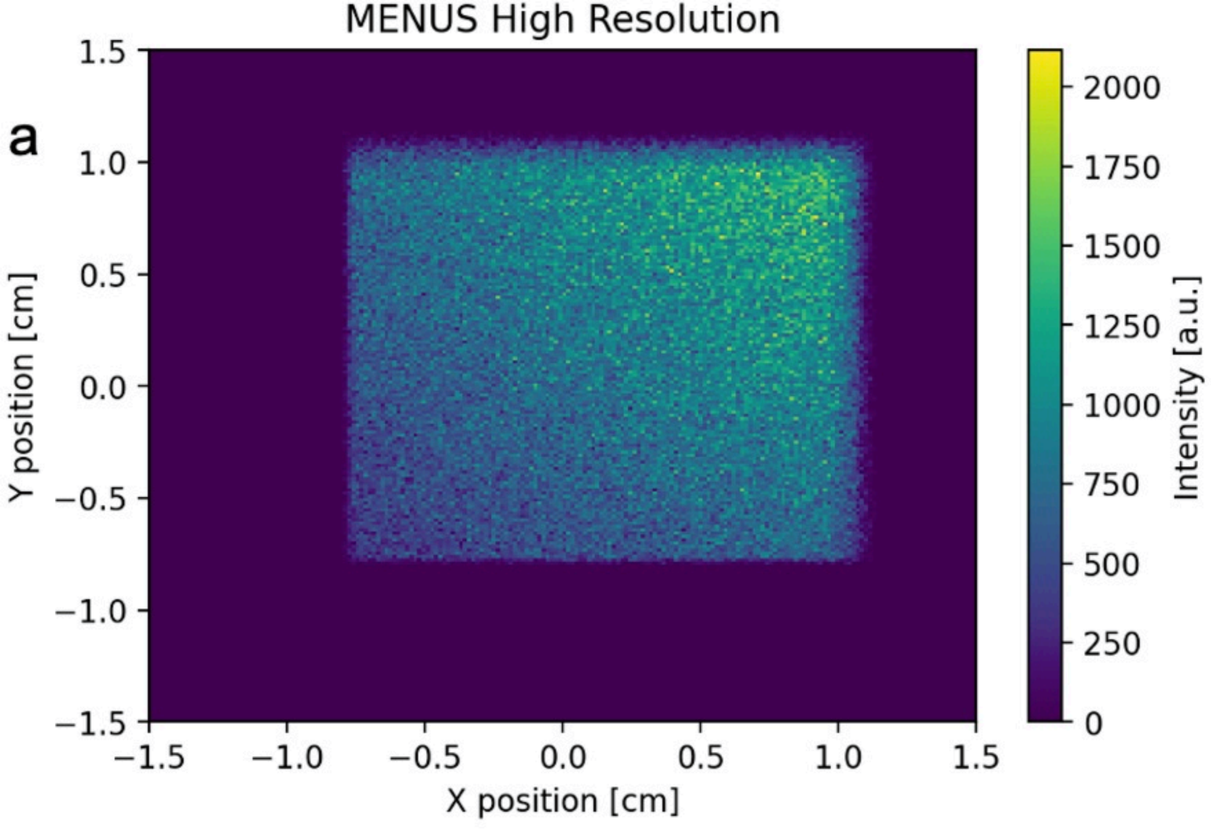
MENUS High Resolution
Y position [cm]
X position [cm]
Intensity [a.u.]
1.5
1.0
0.5
0.0
−0.5
−1.0
−1.5
2000
1750
1500
1250
1000
750
500
250
0

b

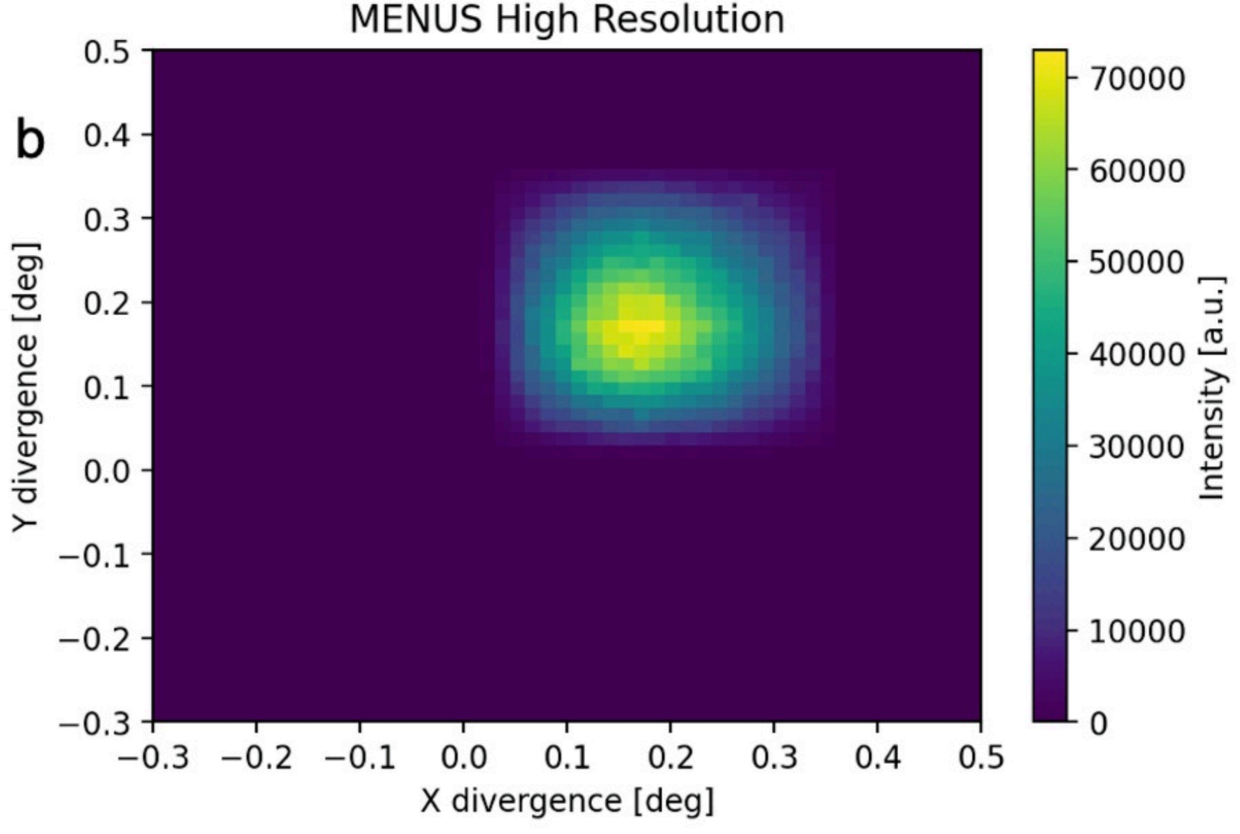
MENUS High Resolution
Y divergence [deg]
X divergence [deg]
Intensity [a.u.]
0.5
0.4
0.3
0.2
0.1
0.0
−0.1
−0.2
−0.3
70000
60000
50000
40000
30000
20000
10000
0

c

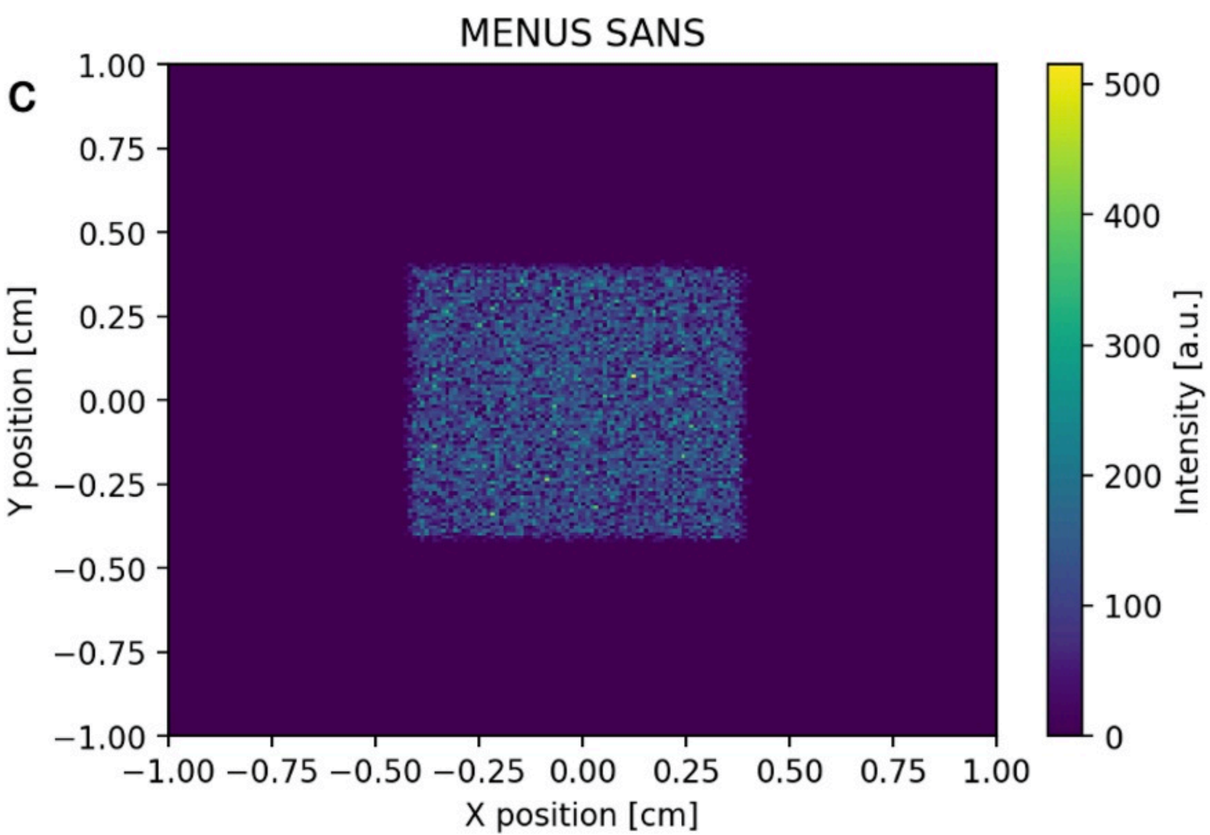
MENUS SANS
Y position [cm]
X position [cm]
Intensity [a.u.]
1.00
0.75
0.50
0.25
0.00
−0.25
−0.50
−0.75
−1.00
500
400
300
200
100
0

d

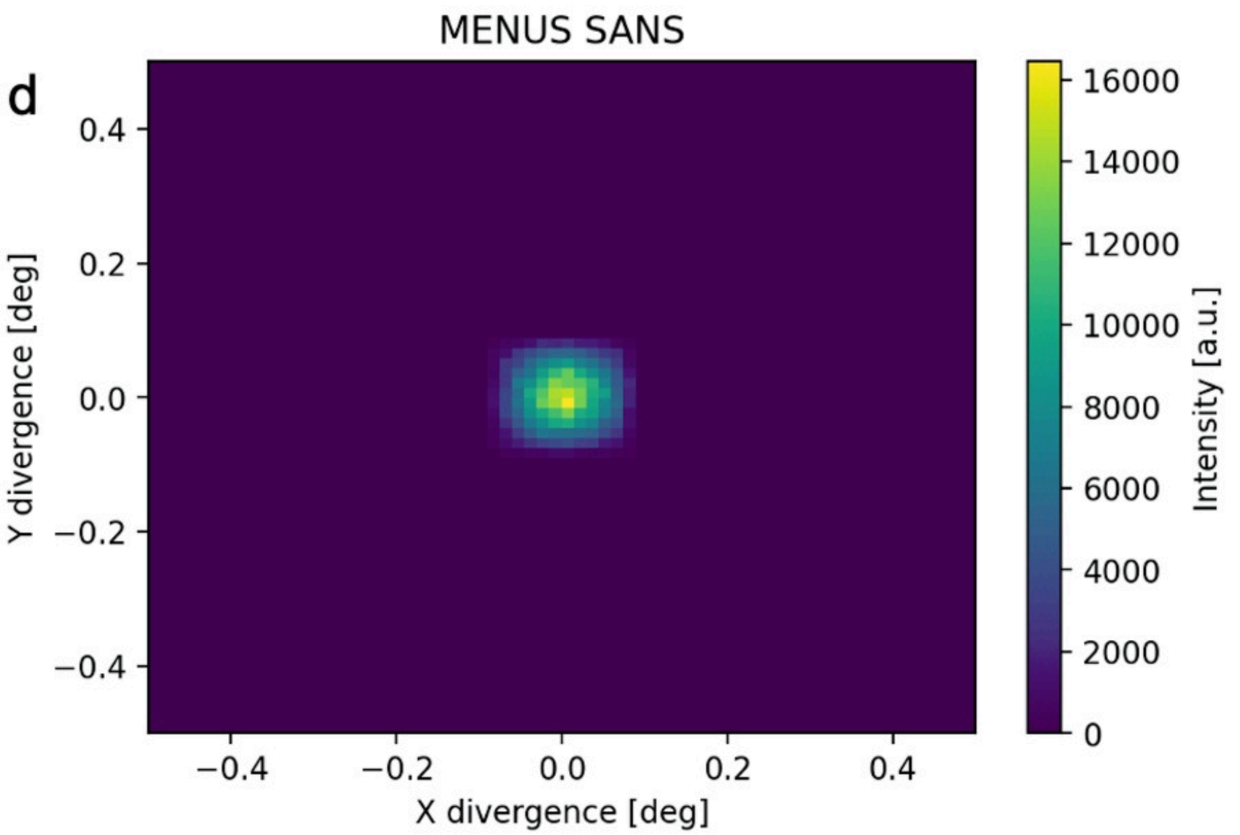
MENUS SANS
Y divergence [deg]
X divergence [deg]
Intensity [a.u.]
0.4
0.2
0.0
−0.2
−0.4
16000
14000
12000
10000
8000
6000
4000
2000
0

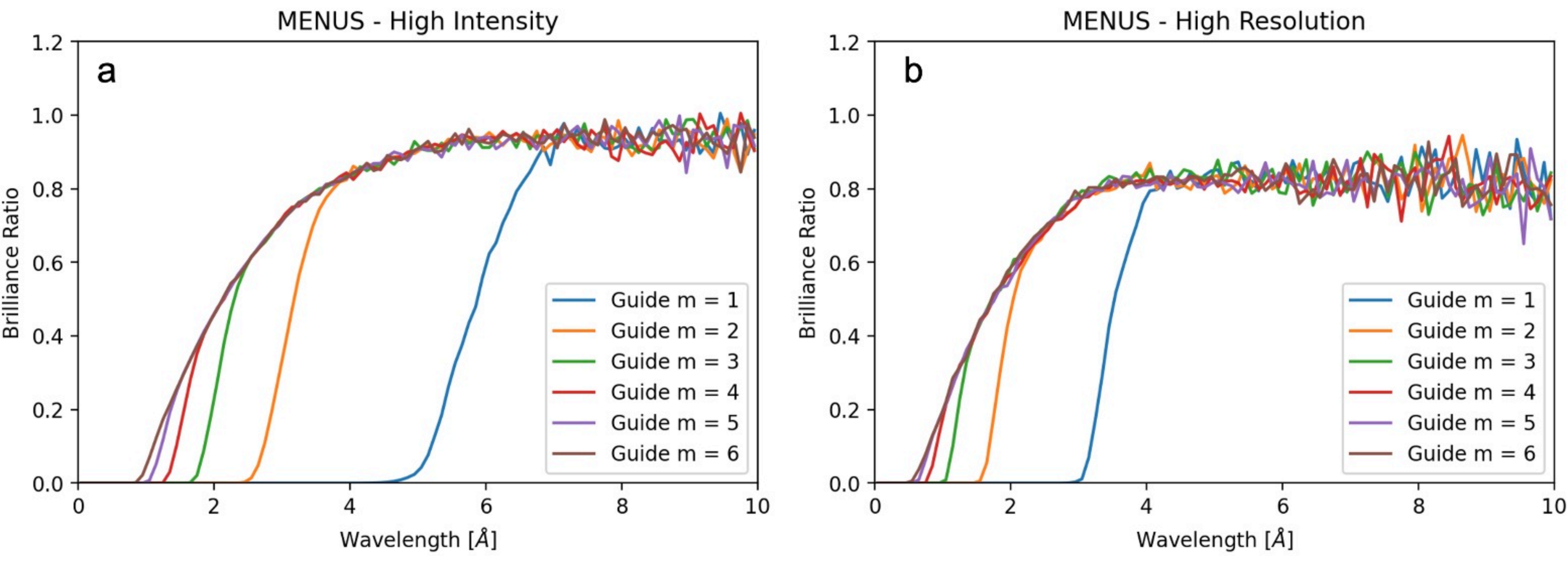
MENUS - High Intensity
a
Brilliance Ratio
Wavelength [Å]
Guide m = 1
Guide m = 2
Guide m = 3
Guide m = 4
Guide m = 5
Guide m = 6
MENUS - High Resolution
b
Brilliance Ratio
Wavelength [Å]
Guide m = 1
Guide m = 2
Guide m = 3
Guide m = 4
Guide m = 5
Guide m = 6

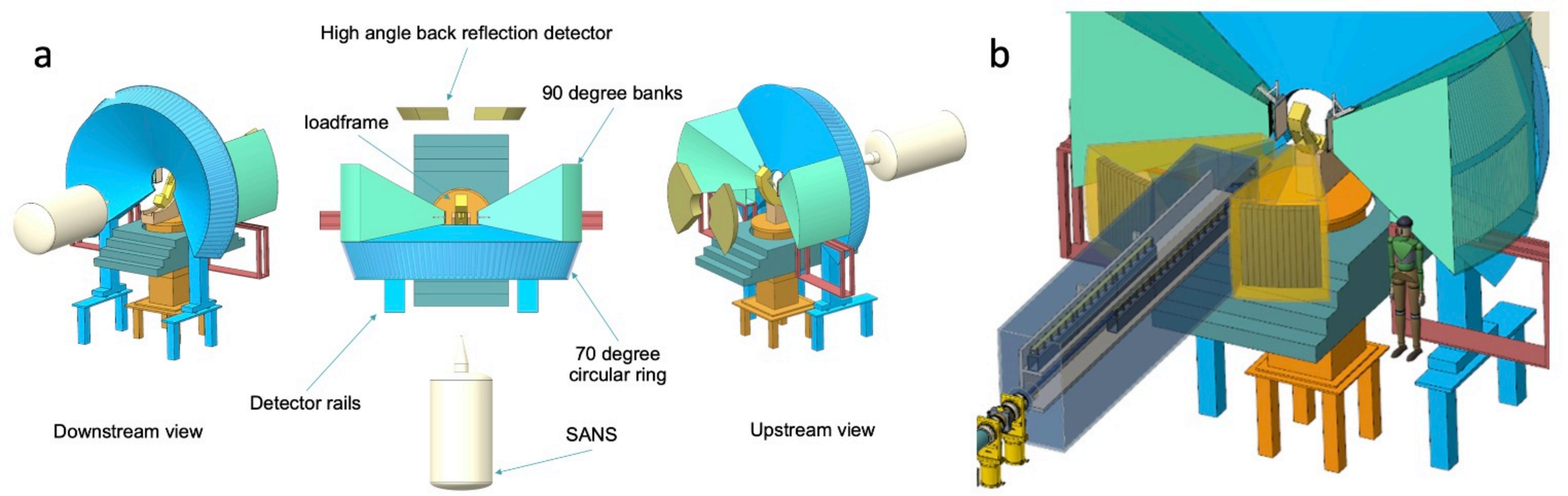
a
High angle back reflection detector
90 degree banks
loadframe
70 degree
circular ring
Detector rails
SANS
Downstream view
Upstream view
b

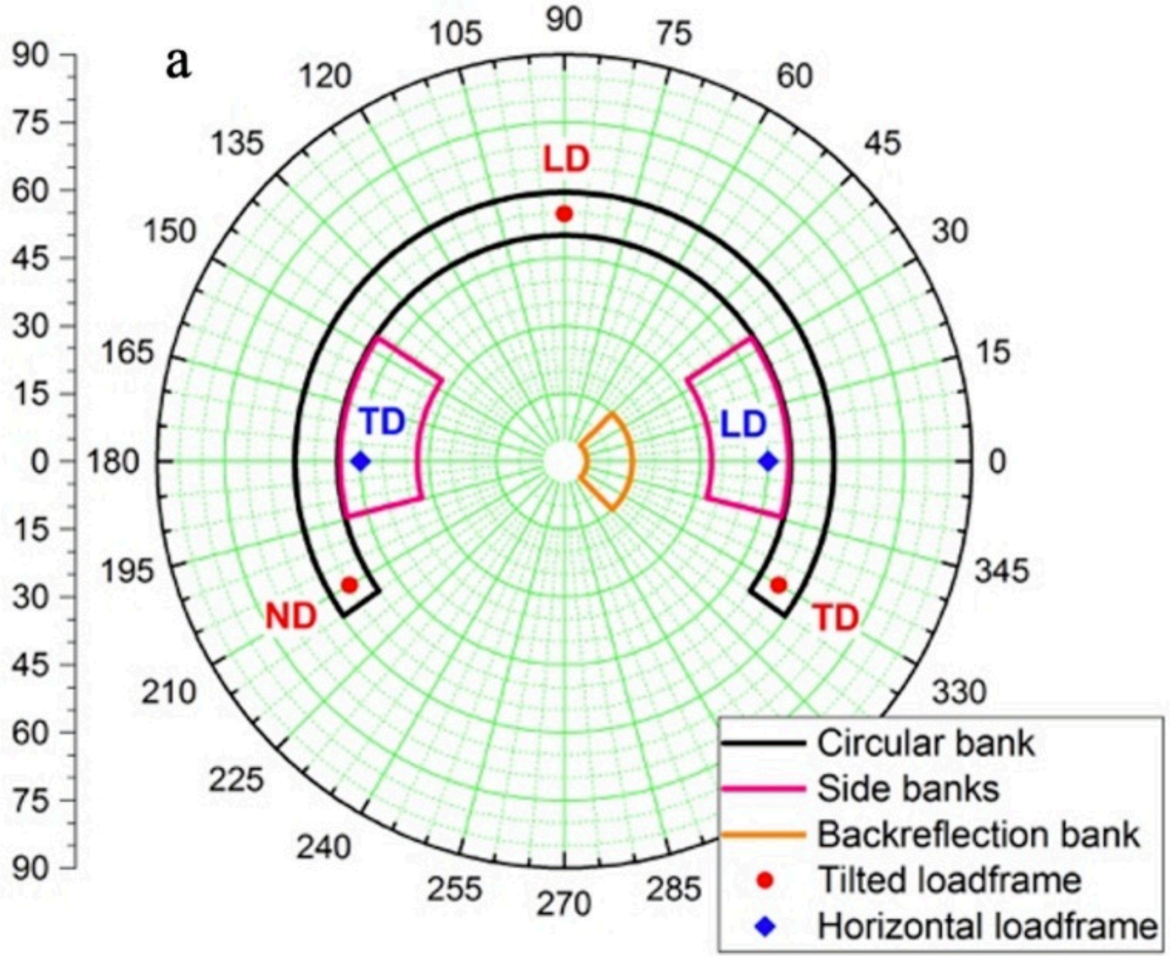
a
LD
TD
LD
ND
TD
Circular bank
Side banks
Backreflection bank
Tilted loadframe
Horizontal loadframe

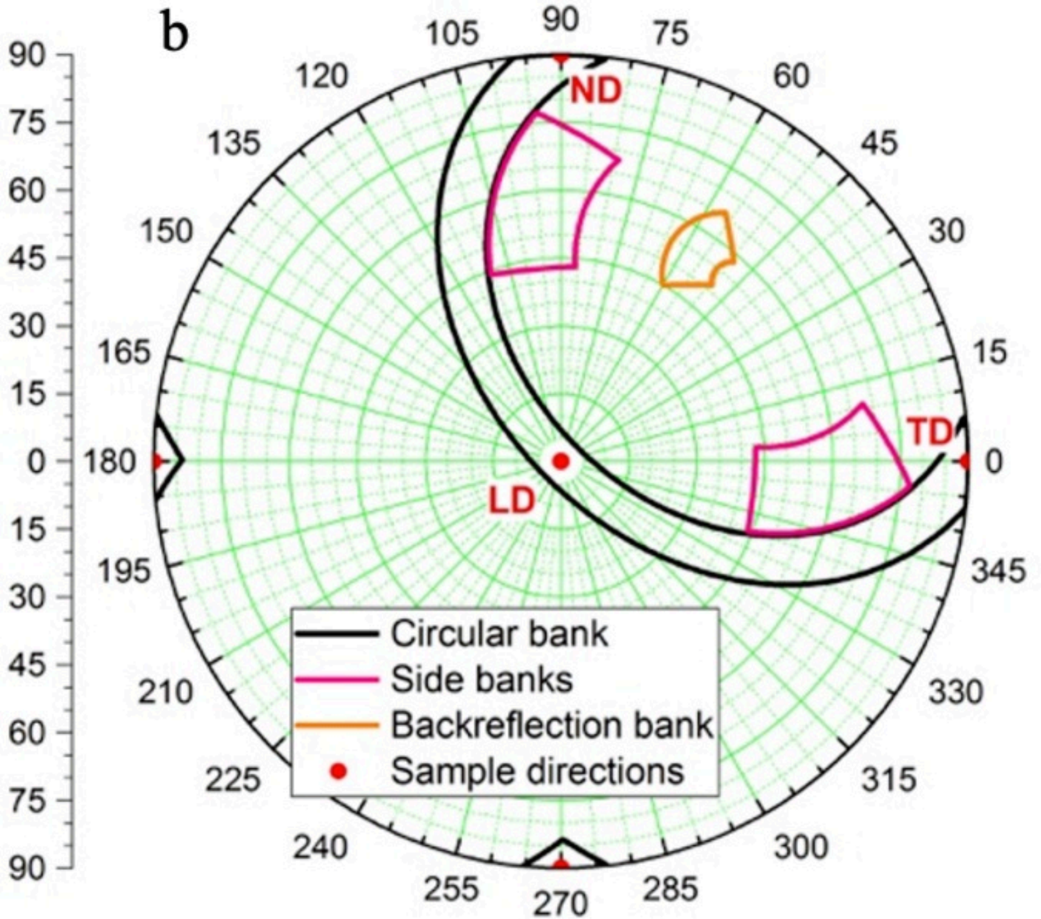
b
ND
LD
TD
Circular bank
Side banks
Backreflection bank
Sample directions

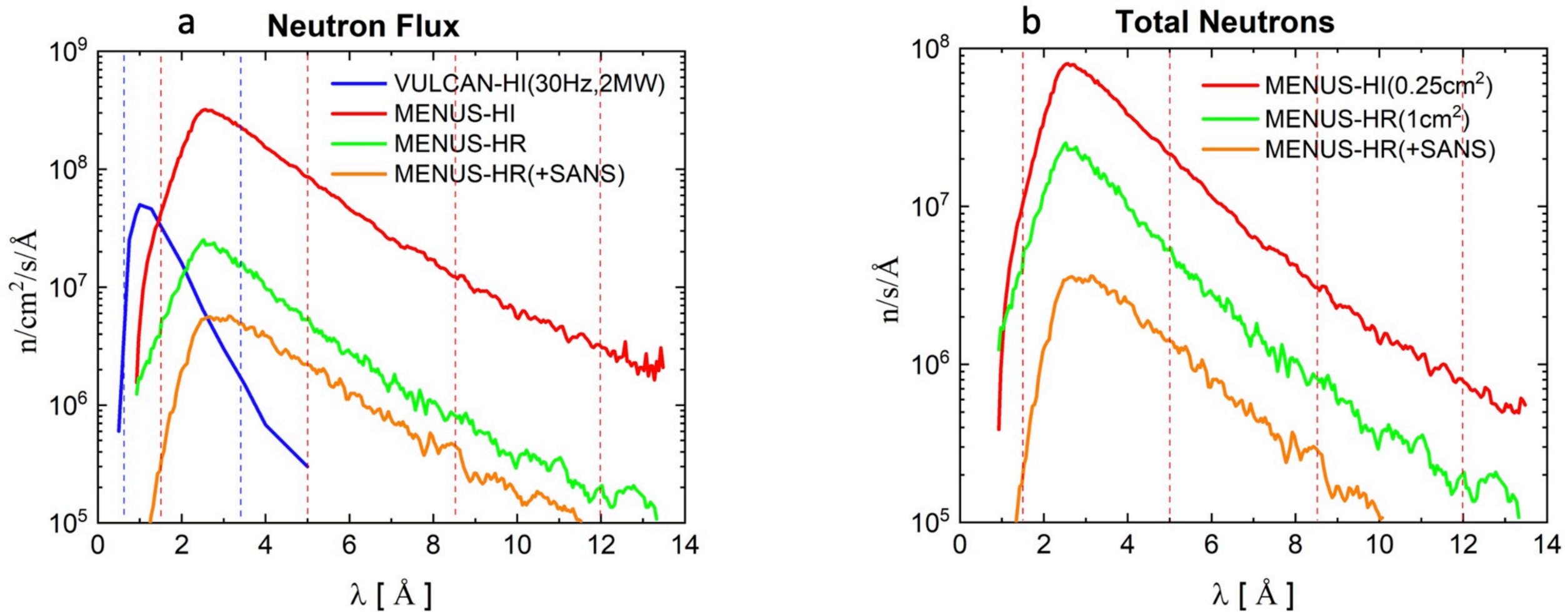
a
Neutron Flux
VULCAN-HI(30Hz,2MW)
MENUS-HI
MENUS-HR
MENUS-HR(+SANS)
n/cm²/s/Å
λ [Å]
b
Total Neutrons
MENUS-HI(0.25cm²)
MENUS-HR(1cm²)
MENUS-HR(+SANS)
n/s/Å
λ [Å]

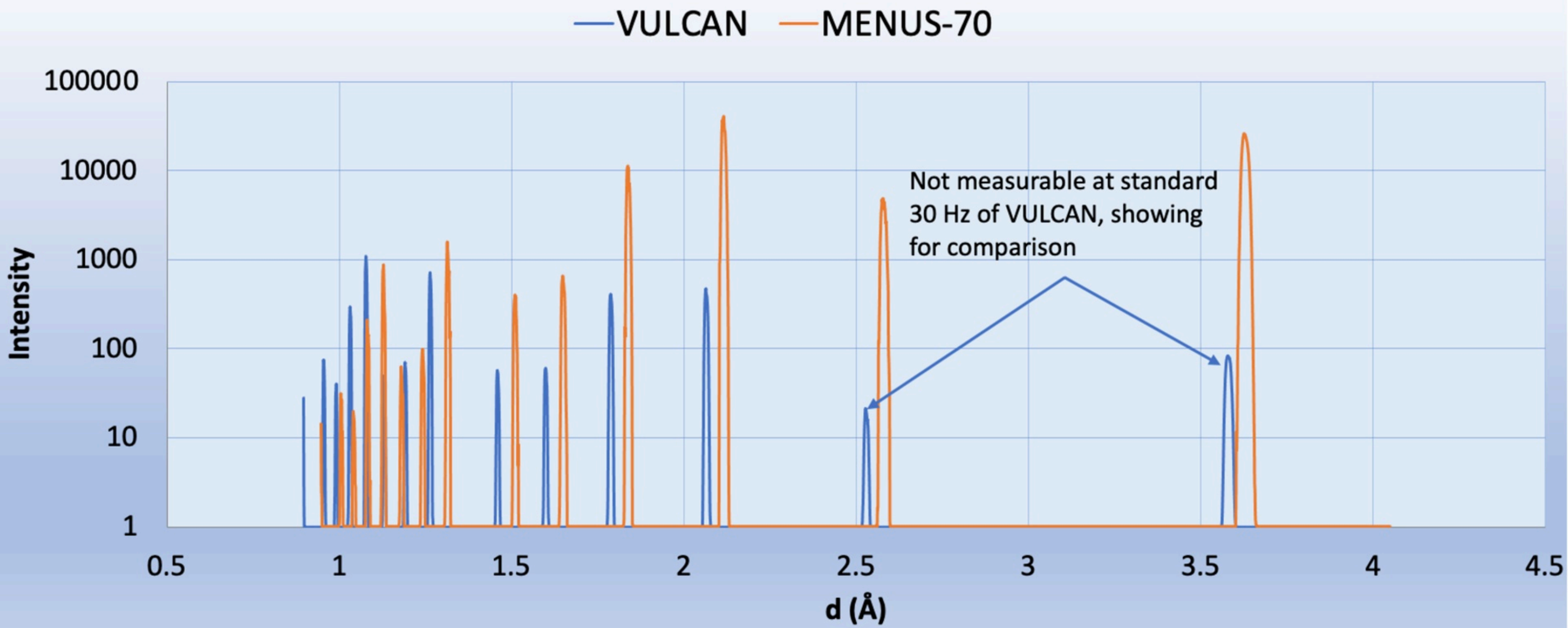
VULCAN
MENUS-70
100000
10000
1000
100
10
1
Intensity
0.5
1
1.5
2
2.5
3
3.5
4
4.5
d (Å)
Not measurable at standard
30 Hz of VULCAN, showing
for comparison

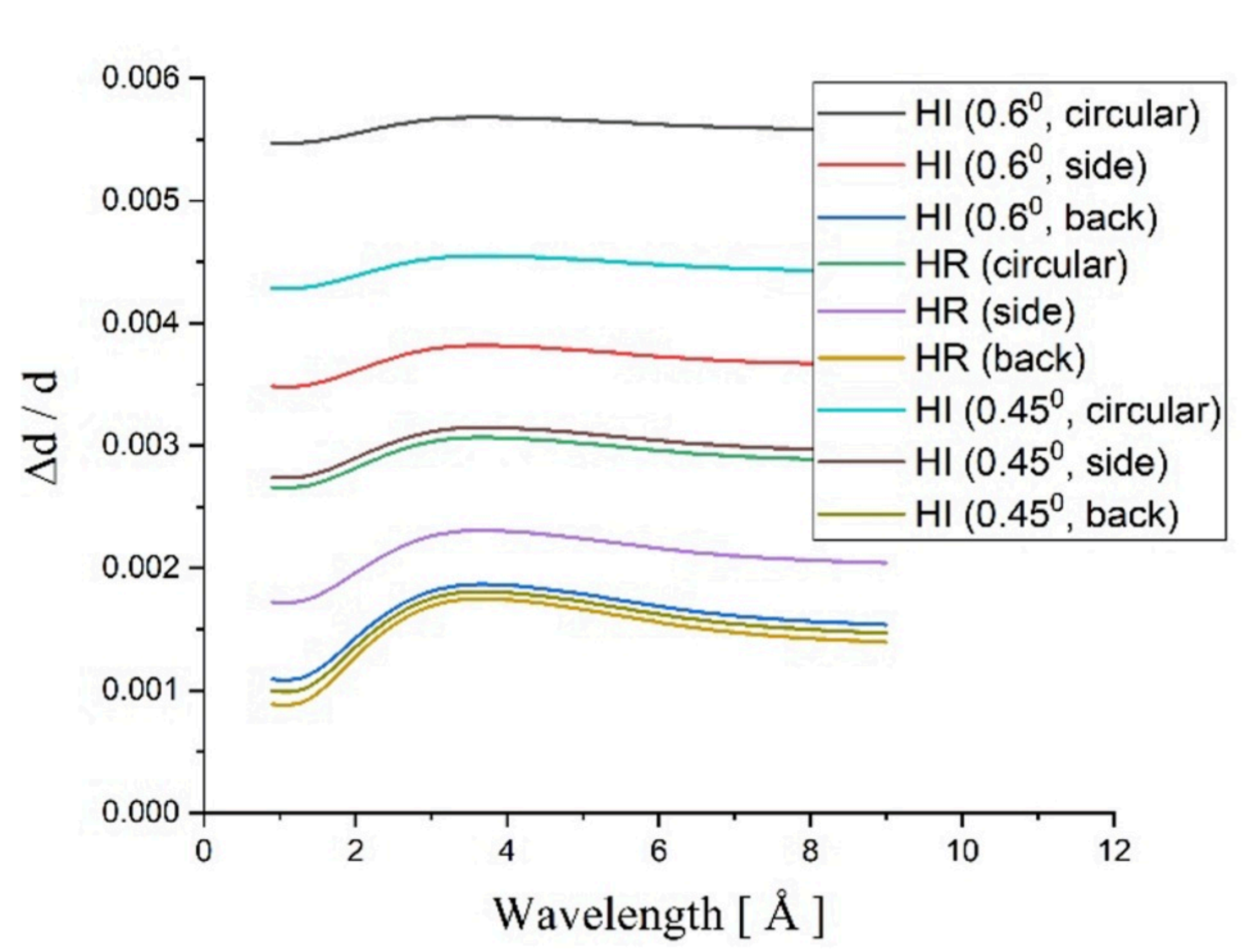
0.006
0.005
0.004
0.003
0.002
0.001
0.000
Δd / d
0
2
4
6
8
10
12
Wavelength [Å]
HI (0.6^0, circular)
HI (0.6^0, side)
HI (0.6^0, back)
HR (circular)
HR (side)
HR (back)
HI (0.45^0, circular)
HI (0.45^0, side)
HI (0.45^0, back)

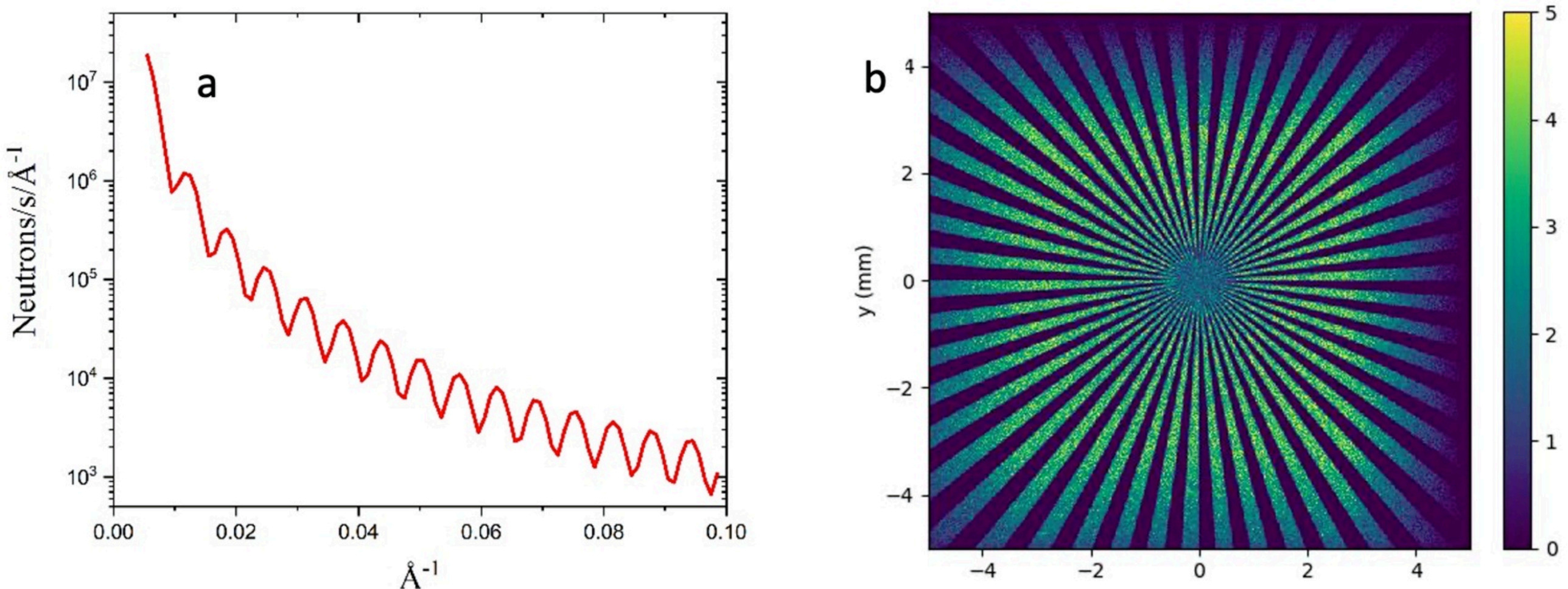
a
Neutrons/s/Å-1
10^7
10^6
10^5
10^4
10^3
0.00
0.02
0.04
0.06
0.08
0.10
Å-1
b
y (mm)
4
2
0
−2
−4
−4
−2
0
2
4
5
4
3
2
1
0